10

Quarks, Gluons, and Jets

The quanta of quantum chromodynamics, 1974–1982.

The striking success of the parton model in describing deep inelastic–nucleon and neutrino–nucleon scattering provided strong circumstantial evidence for the Feynman–Bjorken picture and for its complete elaboration as quantum chromodynamics (QCD). QCD describes all strong interactions as resulting from the interactions of spin-1/2 quarks and spin-1 gluons. The fundamental coupling is of the gluon to the quarks, in a fashion analogous to the coupling of a photon to electrons. In addition, the gluons couple directly to each other. $SU(3)$ plays a central role. Just as in the Gell-Mann–Zweig model of hadrons, there are three basic constituents. The u quark, for example, comes in three versions, say, red, blue, and green. Similarly, every other kind of quark comes in these three versions or "colors." Often it is convenient to refer to u, d, s, and c as "flavors" of quarks, to contrast with the three colors in which every flavor comes. While the $SU(3)$ of flavor is an approximate symmetry, the $SU(3)$ of color is an exact symmetry, thus the three colors of the u quark are exactly degenerate in mass, while the u, d, and s quarks are not degenerate.

The rules of $SU(3)$ state that if we combine a 3 (a quark) with a 3^* (an antiquark), we get $1 + 8$, a singlet and an octet. In terms of mesons, this explains that combining the three quark flavors (u, d, s) with the three antiquark flavors yields an $SU(3)$ singlet (η') and an octet (the pseudoscalar octet of π, K, η). $SU(3)$ color works the same way. Suppose we take red, blue, and green u quarks and combine them with antired, antiblue, and antigreen $\overline{d}$ quarks. We get nine combinations, each of which is $u\overline{d}$. One linear combination is a color singlet and the eight others form a color octet. The gluons are octets of color. From the rule $3 \times 3^* = 1 + 8$ we learn that a quark (3) and an antiquark (3^*) of the same flavor can combine to make a gluon (8).

It was an initial postulate of QCD that only color singlet objects could appear as physical particles. Thus the π^+ would be the color singlet combination of $u\overline{d}$, while the remaining eight combinations would not correspond to physically observed states. Combining three quarks is described by the $SU(3)$ relation $3 \times 3 \times 3 = 1 + 8 + 8 + 10$. When applied to the $SU(3)$ of u, d, and s, this means that baryons should come in 1-, 8-, and 10-dimensional representations. Indeed, these are the representations observed, while mesons

Downloaded from https://www.cambridge.org/core. UNIVERSIDAD AUTONOMA METROPOLITANA, on 19 Nov 2026 at 11:01:57, subject to the Cambridge Core terms of use, available at https://www.cambridge.org/core/terms. https://doi.org/10.1017/9780511609923.012

are not observed in 10-dimensional representations. When applied to color $SU(3)$, the relation shows that there is one way to combine three colors to make a color singlet. This single way corresponds to the antisymmetric combination of the three elements, $rbg - rgb + grb - gbr + bgr - brg$. The combinations producing nonsinglet states do not correspond to physical particles. Indeed an initial impetus for introducing three colors was to explain how the $\Delta^{++}(1232)$ could be a low-lying state. Since it is a uuu and presumably entirely s-wave (as are all lowest-lying states), its wave function is apparently symmetric under interchange of any two quarks. This is not allowed for fermions. A solution to this puzzle was proposed in 1964, before the development of QCD by O. W. Greenberg who added to the other quantum numbers of the quark an index that could take on three values. This index is equivalent to the color quantum number. The color singlet combination of three colors is completely antisymmetric thus making the overall wave function satisfy the Pauli principle.

A single quark cannot be a color singlet and thus should not occur as a physical particle. This property is called "confinement." The quarks are confined inside physical hadrons, which are always color singlets.

The e^+e^- annihilation process produces a virtual photon which according to the quark–parton model couples to the various quarks according to their electric charges. It couples to each color of quark equally. Suppose that the virtual photon produces a $u\overline{u}$ pair that is red–antired. These quarks will be receding from each other rapidly if the energy of the collision is large. Why do they not emerge as isolated quarks? According to QCD, the force between the quarks becomes a constant for large separation. Thus the potential energy is proportional to the separation. When this is large enough, it is energetically favorable to produce a new quark–antiquark pair out of the vacuum, thus reducing the separation between the quark and the antiquark. Suppose this new pair is located so that its antiquark is near the original quark. These may bind to form a meson. The unpaired new quark is still receding from the initial antiquark so it may become favorable to create another new pair. This continues until all the quarks and antiquarks are paired. A similar mechanism permits the creation of baryons.

If the quarks are never free, how can they be observed? Of course they were observed indirectly in deep-inelastic scattering. However, the parton model and QCD indicated that more direct evidence should be obtained by studying certain reactions, the simplest being e^+e^- annihilation. While the produced quarks could not be seen, the initial quarks should materialize into jets of hadrons moving nearly along the directions of the quarks. In a very high energy collision, the hadrons would lie nearly along this single axis, with momenta transverse to it of a few hundred MeV. This estimate was derived from the observation that in most hadronic collisions at high energy, the transverse momentum of the secondaries rarely exceeded this amount.

In an idealized picture, the annihilation of the electron and positron would occur into $\mu^+\mu^-$ pairs and quark–antiquark pairs with frequencies proportional to the squares of the final particle charges. The hadronic final states would come from u, d, and s quarks with probabilities proportional to $3(2/3)^2$, $3(-1/3)^2$, $3(-1/3)^2$, relative to 1 for the muons. The factor 3 arises from the three possible colors. The ratio of the hadronic to muonic final

Downloaded from https://www.cambridge.org/core. UNIVERSIDAD AUTONOMA METROPOLITANA, on 19 Nov 2026 at 11:01:57, subject to the Cambridge Core terms of use, available at https://www.cambridge.org/core/terms. https://doi.org/10.1017/9780511609923.012

states is called R and is thus predicted to be 2 if there are three quarks and three colors. This prediction failed in a spectacular way, as described in the previous chapter. Ultimately, the prediction for R was verified at energies away from the ψ resonances and provided one of the best pieces of evidence for the correctness of QCD. See Fig. 10.1. A second prediction is that the angular distribution of the muons and the quarks should be $1+\cos^2\theta$, relative to the direction of the electron and positron beams. Of course, the direction of the quarks cannot be measured since the quarks are never seen. However, there is an axis for each event, defined by the initial quark direction. This axis is obscured by the transverse momentum acquired by the final-state particles in the "hadronization," in which the initial quarks become hadrons. At sufficiently high energy the axis is clear, but at low energy, the momentum of the final-state particles is not much more than the few hundred MeV anticipated for transverse momentum.

Evidence for jets arising from quarks was first obtained by comparing data taken at various center-of-mass energies (**Ref. 10.1**), using the SLAC–LBL Mark I detector at the SPEAR storage ring located at SLAC. Since the jets could not be discerned by simply looking at the pattern of outgoing tracks, it was necessary to define an algorithm for defining the jet axis. The one selected was that originally proposed by Bjorken and Brodsky. The axis was taken to be the direction such that the sum of the squares of the momenta transverse to the axis was a minimum. For each event, such an axis could be found. Each event was assigned a value of the "sphericity" defined to be

$$S = \frac{3\sum_i \mathbf{p}_{\perp i}^2}{2\sum_i \mathbf{p}_i^2}, \tag{10.1}$$

where $\mathbf{p}_{\perp i}$ is the momentum of the ith particle perpendicular to the sphericity axis. A completely jetlike event with outgoing particles aligned precisely with the axis would have $S = 0$. An isotropic event would have $S \approx 1$. An alternative variable that characterizes e^+e^- events is "thrust." Events with two, well-defined, back-to-back jets have thrust near 1. Spherical events have thrust near 0.

There are two predictions that can be made. First, as the energy increases, the events should become more jetlike so the sphericity should decrease. More importantly, the jet axis should have an angular distribution identical to that for muons. To test the first prediction the sphericity measured at SPEAR was compared at 3.0, 6.2, and 7.4 GeV center-of-mass energy to the predictions of two models, one using an isotropic phase space distribution and one simulating the parton model, with limited transverse momentum relative to the event axis. At 3.0 GeV both models adequately described the sphericity distribution, but at the higher energies only the jetlike parton model succeeded.

Because the Mark I detector was limited in its acceptance in the polar angle, high statistical accuracy was required to test directly the prediction $d\sigma/d\Omega \propto 1+\cos^2\theta$. However, since the beams at SPEAR were polarized at 7.4 GeV, with electron polarization parallel to the magnetic field responsible for the bending of the beams, another approach was available. If the beams were completely polarized, the angular distribution in $e^+e^- \to \mu^+\mu^-$

Downloaded from https://www.cambridge.org/core. UNIVERSIDAD AUTONOMA METROPOLITANA, on 19 Nov 2026 at 11:01:57, subject to the Cambridge Core terms of use, available at https://www.cambridge.org/core/terms. https://doi.org/10.1017/9780511609923.012

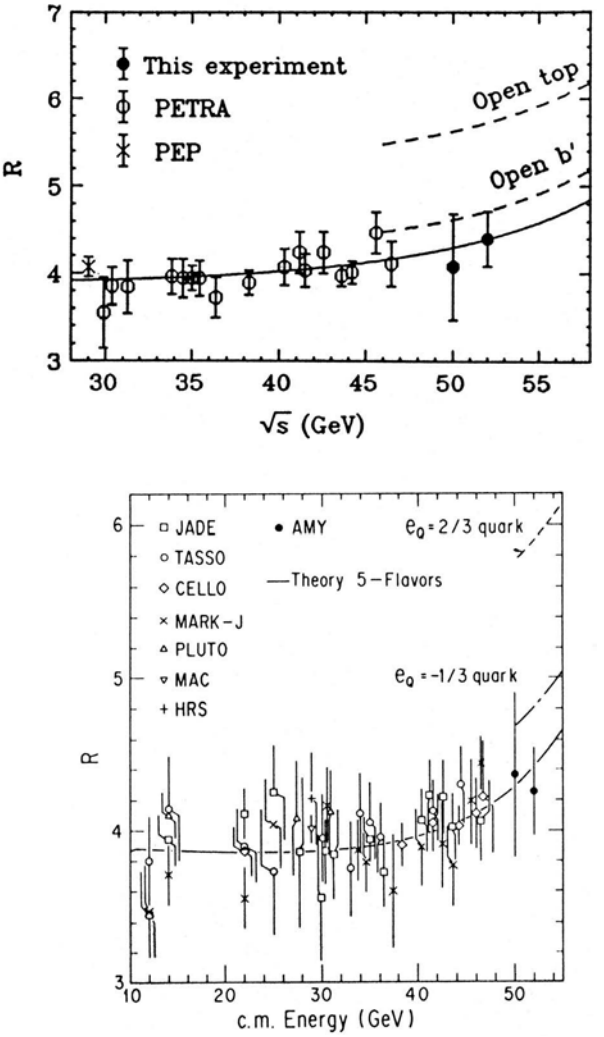


Figure 10.1. Data for e^+e^- annihilation into hadrons as a function of the c.m. energy, including results at $\sqrt{s} = 50$ GeV and 52 GeV from the TRISTAN storage ring located at the KEK Laboratory in Japan: above, results from the TOPAZ Collaboration, [I. Adachi *et al.*, *Phys. Rev. Lett.* **60**, 97 (1988)]; below, results from the AMY Collaboration [H. Sagawa *et al.*, *Phys. Rev. Lett.* **60**, 93 (1988)]. Also shown are results obtained at lower energy machines. The basic prediction of the quark–parton model, including the b-quark discussed in the next Chapter, is $R = 11/3$. QCD radiative corrections and contributions from the Z (discussed in Chapter 12) increase this, and account for the rising prediction at higher c.m. energies. If there were a sixth quark with low enough mass to be pair-produced in this energy region, the value of R would jump as indicated by the curves. Extensive searches at PETRA found no evidence for a sixth quark up to $\sqrt{s} = 46$ GeV. The searches at TRISTAN also show no evidence of a new quark.

Downloaded from https://www.cambridge.org/core. UNIVERSIDAD AUTONOMA METROPOLITANA, on 19 Nov 2026 at 11:01:57, subject to the Cambridge Core terms of use, available at https://www.cambridge.org/core/terms. https://doi.org/10.1017/9780511609923.012

would be

$$d\sigma/d\Omega \propto 1 + \cos^2\theta + \sin^2\theta\cos 2\phi, \tag{10.2}$$

where ϕ is the azimuthal angle measured from the plane of the storage ring. If the degree of polarization of each beam is P, then

$$\begin{aligned} d\sigma/d\Omega &\propto (1-P^2)(1+\cos^2\theta) + P^2(1+\cos^2\theta+\sin^2\theta\cos 2\phi) \\ &\propto 1 + \cos^2\theta + P^2\sin^2\theta\cos 2\phi. \end{aligned} \tag{10.3}$$

This behavior had been confirmed in earlier measurements of the $\mu^+\mu^-$ final state by Mark I at SPEAR. The angular distribution for the hadronic jets would be expected to be the same if the quarks could be regarded as nearly massless spin-1/2 objects with purely pointlike (Dirac) couplings. If, on the other hand, the partons were spin-0, the expected distribution would be

$$d\sigma/d\Omega \propto 1 - \cos^2\theta - P^2\sin^2\theta\cos 2\phi. \tag{10.4}$$

These two cases are the extremes. The Dirac coupling of relativistic spin-1/2 particles to the photon produces a "transverse cross section" in that the electromagnetic current matrix element is perpendicular to the outgoing quark direction, while the coupling of the spin-0 particles to the photon produces a "longitudinal cross section" with the current parallel to the outgoing parton direction. The most general form is

$$d\sigma/d\Omega \propto 1 + \alpha\cos^2\theta + P^2\alpha\sin^2\theta\cos 2\phi, \tag{10.5}$$

where $-1 \le \alpha \le 1$. The square of the polarization was measured to be $P^2 = 0.47 \pm 0.05$ at 7.4 GeV using the $e^+e^- \to \mu^+\mu^-$ process. The hadronic jets gave an angular distribution with $\alpha = 0.45 \pm 0.07$. After correcting for detector effects, this became $\alpha = 0.78 \pm 0.12$ at 7.4 GeV, near the value $\alpha = 1$ predicted for the purely spin-1/2 case. Previously, the Mark I collaboration had measured the angular distribution of produced hadrons, rather than the distribution of the sphericity axis, relative to the beam (Ref. 10.2). There too, the azimuthal dependence indicated that the underlying partons that coupled to the virtual photon produced in e^+e^- annihilation had spin 1/2.

QCD not only encompasses the quark model, it predicts deviations from the simplest form of that model, as discussed in Chapter 8. Deviations from scaling in deep inelastic lepton scattering were predicted using "asymptotic freedom," a property of the theory that states that at high momentum transfer, the coupling between the quarks and the gluons becomes small. This means that in this regime, predictions can be made on the basis of perturbation theory, just as they are in quantum electrodynamics (QED). There are two primary differences. Instead of $\alpha \approx 1/137$, the coupling is $\alpha_s(Q^2)$, a function of the momentum transfer, Q^2. Typically, in the region where perturbation theory applies, $\alpha_s(Q^2) \approx 0.1 - 0.2$. Secondly, unlike photons, gluons can couple to themselves.

Downloaded from https://www.cambridge.org/core. UNIVERSIDAD AUTONOMA METROPOLITANA, on 19 Nov 2026 at 11:01:57, subject to the Cambridge Core terms of use, available at https://www.cambridge.org/core/terms. https://doi.org/10.1017/9780511609923.012

Actually, the α used in QED can also be thought of as a function of the momentum transfer. Because of vacuum polarization, the force between two point charges with separation r is not just α/r^2, but is more accurately $\alpha[1+\alpha f(r)]/r^2$, where $f(r)$ represents the effect of vacuum polarization and is important for r less than the Compton wavelength of the electron. The vacuum polarization in QED increases the force between charges as the distance between them decreases, or equivalently, as the momentum transfer increases. In QCD, the behavior is just the opposite. The coupling gets weaker as the momentum transfer increases. The leading behavior can be expressed as

$$\alpha_s(Q^2) = \frac{4\pi}{(33-2n_f)\ln(Q^2/\Lambda^2)}, \tag{10.6}$$

where n_f is the number of quark flavors (u, d, s, etc.) with mass less than $Q/2$ and Λ is a parameter to be determined experimentally, and is typically found to be about 200 MeV.

The basic process in e^+e^- annihilation into hadrons is, according to the quark–parton model, $e^+e^- \to \gamma^* \to q\overline{q}$. In addition, there are corrections that produce $e^+e^- \to \gamma^* \to q\overline{q}g$, where g is a gluon. The cross section for this is of order α_s relative to the process in which no gluon is produced. It is conventional to define scaled variables $x_i = E_i/E$, where the energies of the $q, \overline{q}$, and g are E_1, E_2, and E_3, and the electron and positron beam energies are E, so that $x_1+x_2+x_3 = 2$. If σ_0 represents the cross section for $e^+e^- \to q\overline{q}$, then

$$\frac{1}{\sigma_0}\frac{d\sigma_{q\overline{q}g}}{dx_1\,dx_2} = \frac{2\alpha_s}{3\pi}\frac{x_1^2+x_2^2}{(1-x_1)(1-x_2)}. \tag{10.7}$$

The cross section is seen to diverge if $x_1 \to 1$ or $x_2 \to 1$. These limits obtain when the gluon is parallel to either the quark or antiquark, or if x_3 goes to zero. If the gluon and the quark are moving in nearly the same direction, it becomes difficult to discern that the gluon is present: the $q\overline{q}g$ state merges into the $q\overline{q}$ state.

While the $q\overline{q}g$ state could be produced at the energy available at SPEAR or DORIS (an e^+e^- collider at DESY with an energy similar to that at SPEAR), we have already seen that the jets in $q\overline{q}$ could just barely be distinguished there. To identify $q\overline{q}g$ states required higher energy. This was achieved first at PETRA, an e^+e^- collider located at DESY, which was able to reach more than 30 GeV total center-of-mass energy.

PETRA had four intersection regions. These were initially occupied by the TASSO, PLUTO, MARK J, and JADE detectors. All found evidence for the $q\overline{q}g$ final state (**Refs. 10.3**, 10.4, 10.5, 10.6). Some data from MARK J, PLUTO, and JADE are shown in Figures 10.2, 10.3, and 10.4. The TASSO collaboration defined three orthogonal axes, $\mathbf{n}_1$, $\mathbf{n}_2$, and $\mathbf{n}_3$, for each event. The direction $\mathbf{n}_3$ was the sphericity axis, the one relative to which the sum of the squares of the transverse momenta was minimal. The direction $\mathbf{n}_1$ maximized the sum of the squares of the transverse momenta. The remaining axis was orthogonal to the other two. The $\mathbf{n}_2$–$\mathbf{n}_3$ plane was thus such that the sum of the squares

Downloaded from https://www.cambridge.org/core. UNIVERSIDAD AUTONOMA METROPOLITANA, on 19 Nov 2026 at 11:01:57, subject to the Cambridge Core terms of use, available at https://www.cambridge.org/core/terms. https://doi.org/10.1017/9780511609923.012

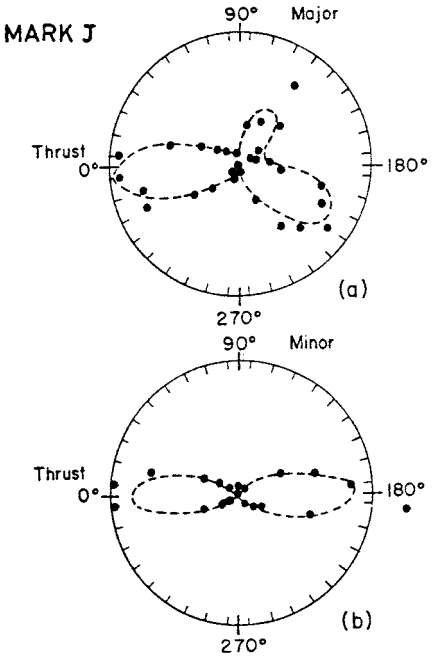


Figure 10.2. Data from the MARK J detector showing the energy flow distribution projected onto a plane. Events showing the typical two-jet distribution are not included. The distance from the center to the data point is proportional to the energy deposited. The dashed line represents the expectation of a $q\overline{q}g$ model. (a) Projection on the plane of the thrust and major axes. (b) Projection on the plane of the thrust and minor axes. The thrust axis is similar to the sphericity axis while the major and minor axes are analogous to the directions $\mathbf{n}_2$ and $\mathbf{n}_1$ defined in the text. (Ref. 10.4)

of the momenta out of it was a minimum. This plane could be viewed as the event plane. Components perpendicular to the primary axis, in and out of the plane were defined:

$$< p_\perp^2 >_{out} = \frac{1}{N}\sum_{j=1}^{N}(\mathbf{p}_j \cdot \mathbf{n}_1)^2 \tag{10.8}$$

$$< p_\perp^2 >_{in} = \frac{1}{N}\sum_{j=1}^{N}(\mathbf{p}_j \cdot \mathbf{n}_2)^2 \tag{10.9}$$

The experiment sought to distinguish between two possibilities. The first was that all $e^+e^- \rightarrow$ hadron events were basically of the form $e^+e^- \rightarrow q\overline{q}$, but as the jet energy increased, the jets became "fatter," i.e. had more transverse momentum relative to the jet axis. The second was that as energy increased, more and more events were due to $e^+e^- \rightarrow q\overline{q}g$. The data showed that at high energies, there were events with $< p_\perp^2 >_{in} >> < p_\perp^2 >_{out}$. This could be understood as the result of $q\overline{q}g$ final states, but not from $q\overline{q}$ final states. Some of the events displayed very clean three-jet topology, providing visual evidence for the existence of the gluon.

Downloaded from https://www.cambridge.org/core. UNIVERSIDAD AUTONOMA METROPOLITANA, on 19 Nov 2026 at 11:01:57, subject to the Cambridge Core terms of use, available at https://www.cambridge.org/core/terms. https://doi.org/10.1017/9780511609923.012

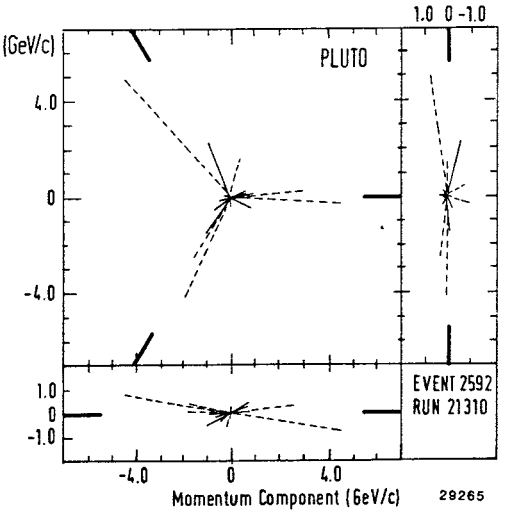


Figure 10.3. Track momentum vectors for a single event observed by the PLUTO collaboration, shown in three projections. The solid lines represent charged particles; the dashed lines, neutral particles. The dark bars show the inferred directions of the three jets. The upper left projection is onto a plane analogous to the $\mathbf{n}_2$–$\mathbf{n}_3$ plane. The bottom projection corresponds to the $\mathbf{n}_1$–$\mathbf{n}_2$ plane and the right projection to the $\mathbf{n}_1$–$\mathbf{n}_3$ plane. (Ref. 10.5)

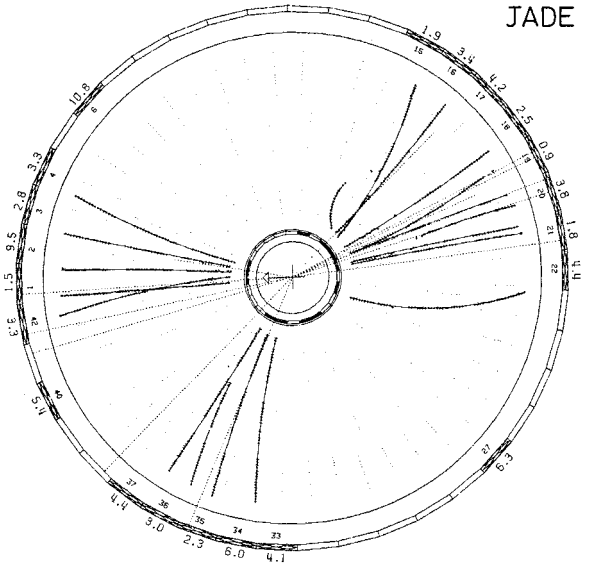


Figure 10.4. A three-jet event measured by the JADE Collaboration, viewed along the beam axis. [P. Söding and G. Wolf, *Ann. Rev. Nucl. Part. Sci.*, **31**, 231 (1981).]

Downloaded from https://www.cambridge.org/core. UNIVERSIDAD AUTONOMA METROPOLITANA, on 19 Nov 2026 at 11:01:57, subject to the Cambridge Core terms of use, available at https://www.cambridge.org/core/terms. https://doi.org/10.1017/9780511609923.012

According to QCD, the fundamental interactions of quarks are due to the exchange of gluons. However, these interactions are obscured because the coupling of the gluons to the quarks is large when the momentum transfer is small. Thus, many gluons are emitted and absorbed in low energy processes. In contrast, at high energies, when the momentum transfer is great, the coupling is small and a single exchange of a gluon may dominate the process.

Experiments at Fermilab, using its 400 GeV proton beam, and the ISR, a proton–proton colliding beam machine at CERN capable of reaching about 60 GeV in the center of mass, sought to identify jets of particles with large transverse momentum. These could arise from the scattering of a quark from the incident proton by a quark from the target proton. The fundamental interaction is the exchange of a gluon between the quarks. This process is entirely analogous to the scattering of alpha particles observed by Geiger and Marsden in 1909. Rutherford inferred from the large angle scattering the existence of a compact, hard nucleus inside the atom. Hadronic jets would support the evidence from electroproduction that inside the nucleon are more fundamental partons, the quarks and gluons. The difficulty was to identify the outgoing jets of particles.

There is no a priori definition that specifies which outgoing particles should be grouped together in identifying a jet. Inevitably, the least energetic particles in a jet merge into the particles not associated with the jet. It is necessary in each experiment to set out an algorithm that defines a jet. This is an especially serious problem at lower energies where jet structures are not clear. Despite years of determined effort, the results from Fermilab and the ISR were not conclusive but only suggestive of jets.

With the operation of the Sp$\overline{\text{p}}$S Collider at CERN, the energies available increased enormously, to $\sqrt{s} = 540$ GeV. Two large detectors, UA-1 and UA-2, were prepared to measure the anticipated high transverse momentum events with highly segmented calorimeters.

Early results from the UA-2 detector showed unambiguous evidence for large transverse momentum jets (**Ref. 10.7**). The UA-2 detector featured one set of calorimeters covering from 40° to 140° in polar angle and a second set covering from 20° to 37.5° and from 142.5° to 160°. The azimuthal coverage in the central region was 300° and consisted of 200 cells.

Since transverse momentum is the signal of interest, the energy measurements are converted to "transverse energy," $E_T = E \sin\theta$, where θ is the polar angle between the beam direction and the jet, and E is the energy deposited into some portion of the detector. In lower energy experiments events with large total transverse energy ΣE_T were observed, but often the transverse energy was not localized into two distinct directions representing two jets, but rather was spread over a large portion of the total solid angle. The UA-2 collaboration was able to provide evidence for well-defined jets at the high energy offered by the Sp$\overline{\text{p}}$S Collider.

To give an operational definition of a jet, the UA-2 collaboration defined a "cluster" of calorimeter cells as a set of contiguous cells each showing an energy deposit greater than 400 MeV. It was then found that as ΣE_T increased, a larger and larger fraction of the total was contained in the two clusters having the largest E_T. This was quite clear evidence for the long-sought-for jets. Some individual events showed strikingly clear evidence for the

Downloaded from https://www.cambridge.org/core. UNIVERSIDAD AUTONOMA METROPOLITANA, on 19 Nov 2026 at 11:01:57, subject to the Cambridge Core terms of use, available at https://www.cambridge.org/core/terms. https://doi.org/10.1017/9780511609923.012

jets, which could be displayed in "Lego" plots showing the energy deposited in the various calorimeter cells. A series of comparisons showed qualitative agreement with the two-jet picture.

The measured distributions for high-transverse-momentum jets was in reasonable agreement with predictions made from QCD-based models. These models used quark and gluon distributions derived from deep inelastic scattering, together with cross sections calculated from perturbative QCD for the processes like $q\overline{q} \to q\overline{q}$ and $gq \to gq$. The fastest partons in a proton are quarks, so the very high transverse momentum events should arise from the $q\overline{q} \to q\overline{q}$ process. However, the cross sections for these events are small. At more modest transverse momenta, where there are more events, it is actually $gg \to gg$ that is expected to dominate. This is so because of the large number of gluons in the structure functions at high Q^2 and at not too large x, and because the coupling of gluons to other gluons is stronger than the coupling of gluons to quarks.

While high-precision tests were lacking, the qualitative features of the jets found at SPEAR, PETRA, and the Sp$\overline{\text{p}}$S Collider confirmed the general predictions of QCD and established its applicability in both leptonically and hadronically induced processes.

Exercises

10.1 Using numerical methods, determine the fraction of e^+e^- events that produce $q\overline{q}g$, where $x_1, x_2, x_3 < 0.9$. Suppose it is also required that $E_1, E_2, E_3 > 5$ GeV. What fraction of $e^+e^- \to$ hadrons events at $E_{cm} = 30, 60, 90$ GeV satisfy this condition as well? Take $\alpha_s = 0.1$.

10.2 Consider the cross section for qq scattering if the quarks are of different flavors (e.g. u and d). The gluon coupling to quarks is completely analogous to the photon coupling with electrons, except that there is a matrix specifying the color interaction:

$$g_s \overline{q}_a \frac{1}{2} \lambda_i^{ab} \gamma_\mu q_b,$$

where $a, b = 1, 2, 3$. The λ_is, $i = 1, \ldots, 8$ are 3×3 traceless matrices satisfying

$$\text{Tr}\lambda_i \lambda_j = 2\delta_{ij} \qquad i, j = 1, \ldots 8,$$

and $g_s^2 = 4\pi\alpha_s$. Find $d\sigma/d\Omega$ for the elastic scattering relative to what it would be without color factors, remembering to average over initial states and sum over final states.

10.3 Suppose the color gauge group were $SO(3)$ (the rotation group) instead of $SU(3)$ and suppose that the quarks came in three colors corresponding to the three-dimensional (vector) representation of $SO(3)$. Assume that hadrons must still be color singlets. Why would this not produce just the usual mesons and baryons?

Downloaded from https://www.cambridge.org/core. UNIVERSIDAD AUTONOMA METROPOLITANA, on 19 Nov 2026 at 11:01:57, subject to the Cambridge Core terms of use, available at https://www.cambridge.org/core/terms. https://doi.org/10.1017/9780511609923.012

10.4 * Verify that if the electrons and positrons are completely polarized with their spins perpendicular to the plane of the ring (antiparallel to each other), the angular distribution for $e^+e^- \to \mu^+\mu^-$ is

$$d\sigma/d\Omega \propto 1 + \cos^2\theta + \sin^2\theta \cos 2\phi$$

where θ measures the polar angle away from the beam direction and ϕ the azimuthal angle from the plane of the ring. [Consider the matrix element for producing the virtual photon, $\mathcal{M} \propto \overline{v}\epsilon_\mu \gamma^\mu u$, where ϵ is the polarization vector of the virtual photon and show that if the electron and positron spins are perpendicular to the plane of the ring, so is ϵ. Then consider the matrix element for the decay into massless fermions, $\mathcal{M} \propto \overline{u}(k)\epsilon_\mu \gamma^\mu v(k')$ and calculate $|\mathcal{M}|^2$, summing over final-state spins to find the angular distribution.] Do the same for the final state with two spin-0 particles. The decay matrix element is proportional to $(k-k')_\mu \epsilon^\mu$, where k and k' are the final-state momenta.

Further Reading

Extensive coverage of QCD is given in C. Quigg, *Gauge Theories of the Strong, Weak, and Electromagnetic Interactions*, Benjamin/Cummings, Menlo Park, CA, 1983, and Westview Press, 1997. See especially Chapter 8.

A comprehensive treatment is given in R. K. Ellis, W. J. Stirling, and B. R. Webber, *QCD and Collider Physics,* Cambridge University Press, 1996.

The polarization of electron and positron beams in storage rings caused by spin-flip emission of synchrotron radiation is beautifully explained in J. D. Jackson, *Rev. Mod. Phys.* **48**, 417 (1976).

References

10.1 G. Hanson *et al.*, "Evidence for Jet Structure in Hadron Production by e^+e^- Annihilation." *Phys. Rev. Lett.*, **35**, 1609 (1975).
10.2 R. F. Schwitters *et al.*, "Azimuthal Asymmetry in Inclusive Hadron Production by e^+e^- Annihilation." *Phys. Rev. Lett.*, **35**, 1320 (1975).
10.3 TASSO Collaboration, R. Brandelik *et al.*, "Evidence for Planar Events in e^+e^- Annihilation at High Energies." *Phys. Lett.*, **86B**, 243 (1979).
10.4 MARK J Collaboration, D. P. Barber *et al.*, "Discovery of Three-jet Events and a Test of Quantum Chromodynamics at PETRA." *Phys. Rev. Lett.*, **43**, 830 (1979).
10.5 PLUTO Collaboration, Ch. Berger *et al.*, "Evidence for Gluon Bremsstrahlung in e^+e^- Annihilation at High Energies." *Phys. Lett.*, **86B**, 418 (1979).
10.6 JADE Collaboration, W. Bartel *et al.*, "Observation of Planar Three-jet Events in e^+e^- Annihilation and Evidence for Gluon Bremsstrahlung." *Phys. Lett.*, **91B**, 142 (1980).
10.7 UA-2 Collaboration, M. Banner *et al.*, "Observation of Very Large Transverse Momentum Jets at the CERN $\overline{\text{p}}\text{p}$ Collider." *Phys. Lett.*, **118B**, 203 (1982).

Downloaded from https://www.cambridge.org/core. UNIVERSIDAD AUTONOMA METROPOLITANA, on 19 Nov 2026 at 11:01:57, subject to the Cambridge Core terms of use, available at https://www.cambridge.org/core/terms. https://doi.org/10.1017/9780511609923.012

VOLUME 35, NUMBER 24 PHYSICAL REVIEW LETTERS 15 DECEMBER 1975

Evidence for Jet Structure in Hadron Production by e^+e^- Annihilation*

G. Hanson, G. S. Abrams, A. M. Boyarski, M. Breidenbach, F. Bulos, W. Chinowsky, G. J. Feldman, C. E. Friedberg, D. Fryberger, G. Goldhaber, D. L. Hartill,† B. Jean-Marie, J. A. Kadyk, R. R. Larsen, A. M. Litke, D. Lüke,‡ B. A. Lulu, V. Lüth, H. L. Lynch, C. C. Morehouse, J. M. Paterson, M. L. Perl, F. M. Pierre,§ T. P. Pun, P. A. Rapidis, B. Richter, B. Sadoulet, R. F. Schwitters, W. Tanenbaum, G. H. Trilling, F. Vannucci,‖ J. S. Whitaker, F. C. Winkelmann, and J. E. Wiss

Lawrence Berkeley Laboratory and Department of Physics, University of California, Berkeley, California 94720, and Stanford Linear Accelerator Center, Stanford University, Stanford, California 94305

(Received 8 October 1975)

We have found evidence for jet structure in $e^+e^- \rightarrow$ hadrons at center-of-mass energies of 6.2 and 7.4 GeV. At 7.4 GeV the jet-axis angular distribution integrated over azimuthal angle was determined to be proportional to $1+(0.78\pm0.12)\cos^2\theta$.

In quark-parton constituent models of elementary particles, hadron production in e^+e^- annihilation reactions proceeds through the annihilation of the e^+ and e^- into a virtual photon which subsequently produces a quark-parton pair, each member of which decays into hadrons. At sufficiently high energy the limited transverse-momentum distribution of the hadrons with respect to the original parton production direction, characteristic of all strong interactions, results in oppositely directed jets of hadrons.[1-4] The spins of the constituents can, in principle, be determined from the angular distribution of the jets. In this Letter we report the evidence for the existence of jets and the angular distribution of the jet axis.

The data were taken with the Stanford Linear Accelerator Center–Lawrence Berkeley Laboratory magnetic detector at the SPEAR storage ring of the Stanford Linear Accelerator Center. Hadron production, muon pair production, and Bhabha scattering data were recorded simultaneously. The detector and the selection of events have been described previously.[5,6] The detector subtended $0.65\times 4\pi$ sr with full acceptance in azimuthal angle and acceptance in polar angle from

Downloaded from https://www.cambridge.org/core. UNIVERSIDAD AUTONOMA METROPOLITANA, on 19 Nov 2026 at 11:01:57, subject to the Cambridge Core terms of use, available at https://www.cambridge.org/core/terms. https://doi.org/10.1017/9780511609923.012

50° to 130°. We have used the large blocks of data at center-of-mass energies ($E_{c.m.}$) of 3.0, 3.8, 4.8, 6.2, and 7.4 GeV. We included only those hadronic events in which three or more particles were detected in order to avoid background contamination in events with only two charged tracks due to beam-gas interactions and photon-photon processes.

To search for jets we find for each event that direction which minimizes the sum of squares of transverse momenta.[7] For each event we calculate the tensor

$$T^{\alpha\beta} = \sum_i (\delta^{\alpha\beta}\vec{p}_i^{\,2} - p_i^{\alpha} p_i^{\beta}), \quad (1)$$

where the summation is over all detected particles and α and β refer to the three spatial components of each particle momentum $\vec{p}_i$. We diagonalize $T^{\alpha\beta}$ to obtain the eigenvalues λ_1, λ_2, and λ_3 which are the sums of squares of transverse momenta with respect to the three eigenvector directions. The smallest eigenvalue (λ_3) is the minimum sum of squares of transverse momenta. The eigenvector associated with λ_3 is defined to be the reconstructed jet axis. In order to determine how jetlike an event is, we calculate a quantity which we call the sphericity (S):

$$S = \frac{3\lambda_3}{\lambda_1+\lambda_2+\lambda_3} = \frac{3(\sum_i p_{\perp i}^2)_{\min}}{2\sum_i \vec{p}_i^{\,2}}. \quad (2)$$

S approaches 0 for events with bounded transverse momenta and approaches 1 for events with large multiplicity and isotropic phase-space particle distributions.

The data at each energy were compared to Monte Carlo simulations which were based on either an isotropic phase-space (PS) model or a jet model. In both models only pions (charged and neutral) were produced. The total multiplicity was given by a Poisson distribution. The jet model modified phase space according to the square of a matrix element of the form

$$M^2 = \exp(-\textstyle\sum_i p_{\perp i}^2/2b^2), \quad (3)$$

where $p_\perp$ is the momentum perpendicular to the jet axis.

The angular distribution for the jet axis is expected to have the form

$$d\sigma/d\Omega \propto 1 + \alpha\cos^2\theta + P^2\alpha\sin^2\theta\cos(2\varphi), \quad (4)$$

where θ is the polar angle of the jet axis with respect to the incident positron direction, φ is the azimuthal angle with respect to the plane of the storage ring, $\alpha = (\sigma_T - \sigma_L)/(\sigma_T + \sigma_L)$ with σ_T and σ_L the transverse and longitudinal production cross sections, and P is the polarization of each beam. (The polarization term will be discussed later.) The angular distribution given by Eq. (4) was used in the jet-model simulation. The simulations included the geometric acceptance, the trigger efficiency, and all other known characteristics of the detector. The total multiplicity and the charged-neutral multiplicity ratio for both models were obtained by fitting to the observed charged-particle mean multiplicity and mean momentum at each energy. In the jet model the parameter b was determined by fitting to the observed mean S at the highest energy (7.4 GeV). For lower energies the value of b was determined by requiring that the mean $p_\perp$ in the jet model be the same (315 MeV/c) as at 7.4 GeV.

Figure 1 shows the observed mean S and the model predictions. Both models are consistent with the data in the 3–4-GeV region. At higher energies the data have significantly lower mean S than the PS model and agree with the jet model. Figure 2 shows the S distributions at several energies. At 3.0 GeV the data agree with either the PS or the jet model [Fig. 2(a)]. At 6.2 and 7.4 GeV the data are peaked toward low S, favoring

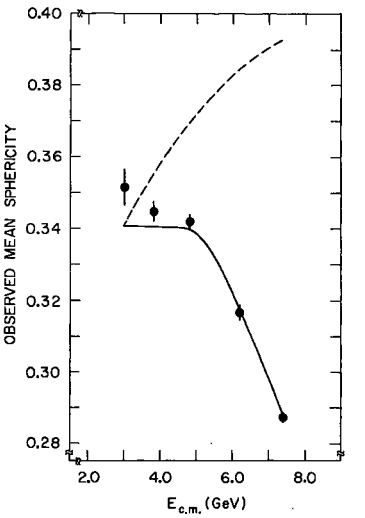


FIG. 1. Observed mean sphericity versus center-of-mass energy $E_{c.m.}$ for data, jet model with $\langle p_\perp \rangle = 315$ MeV/c (solid curve), and phase-space model (dashed curve).

Downloaded from https://www.cambridge.org/core. UNIVERSIDAD AUTONOMA METROPOLITANA, on 19 Nov 2026 at 11:01:57, subject to the Cambridge Core terms of use, available at https://www.cambridge.org/core/terms. https://doi.org/10.1017/9780511609923.012

VOLUME 35, NUMBER 24 PHYSICAL REVIEW LETTERS 15 DECEMBER 1975

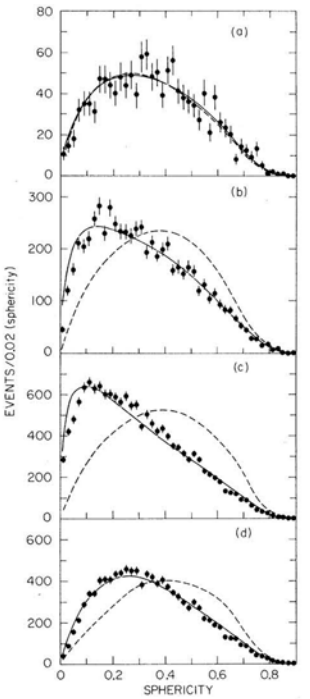


FIG. 2. Observed sphericity distributions for data, jet model with $\langle p_\perp \rangle = 315$ MeV/c (solid curves), and phase-space model (dashed curves) for (a) $E_{c.m.} = 3.0$ GeV; (b) $E_{c.m.} = 6.2$ GeV; (c) $E_{c.m.} = 7.4$ GeV; and (d) $E_{c.m.} = 7.4$ GeV, events with largest $x < 0.4$. The distributions for the Monte Carlo models are normalized to the number of events in the data.

the jet model [Figs. 2(b) and 2(c)]. At the highest two energies, the PS model poorly reproduces the single-particle momentum spectra, having fewer particles with $x > 0.4$ ($x = 2p/E_{c.m.}$ and p is the particle momentum) than the data.[8] The jet-model x distributions are in better agreement. For $x < 0.4$ the x distributions for both models agree with the data. Therefore, we show in Fig. 2(d) the S distributions at 7.4 GeV for those events in which *no* particle has $x > 0.4$. The jet model is still preferred.

At $E_{c.m.} = 7.4$ GeV the electron and positron beams in the SPEAR ring are transversely polarized, and the hadron inclusive distributions show an azimuthal asymmetry.[9] The φ distributions of the jet axis for jet axes with $|\cos\theta| \leq 0.6$ are shown in Fig. 3 for 6.2 and 7.4 GeV.[10] At 6.2

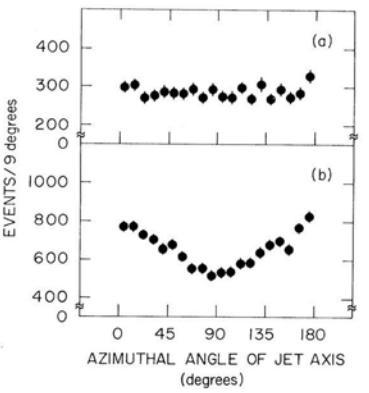


FIG. 3. Observed distributions of jet-axis azimuthal angles from the plane of the storage ring for jet axes with $|\cos\theta| \leq 0.6$ for (a) $E_{c.m.} = 6.2$ GeV and (b) $E_{c.m.} = 7.4$ GeV.

GeV, the beams are unpolarized[9] and the φ distribution is flat, as expected. At 7.4 GeV, the φ distribution of the jet axis shows an asymmetry with maxima and minima at the same values of φ as for $e^+e^- \to \mu^+\mu^-$.

The φ distribution shown in Fig. 3(b) and the value for P^2 (0.47 ± 0.05) measured simultaneously by the reaction[9] $e^+e^- \to \mu^+\mu^-$ were used to determine the parameter α of Eq. (4). The value obtained for the *observed* jet axis is $\alpha = 0.45 \pm 0.07$. This observed value of α will be less than the true value which describes the production of the jets because of the incomplete acceptance of the detector, the loss of neutral particles, and our method of reconstructing the jet axis. We have used the jet-model Monte Carlo simulation to estimate the ratio of observed to produced values of α and find this ratio to be 0.58 at 74 GeV. Thus the value of α describing the *produced* jet-axis angular distribution is $\alpha = 0.78 \pm 0.12$ at $E_{c.m.} = 7.4$ GeV. The error in α is statistical only; we estimate that the systematic errors in the observed α can be neglected. However, we have not studied the model dependence of the correction factor relating observed to produced values of α.

The sphericity and the value of α as determined above are properties of whole events. The simple jet model used for the sphericity analysis can also be used to predict the single-particle inclusive angular distributions for all values of the secondary particle momentum. In Fig.

Downloaded from https://www.cambridge.org/core. UNIVERSIDAD AUTONOMA METROPOLITANA, on 19 Nov 2026 at 11:01:57, subject to the Cambridge Core terms of use, available at https://www.cambridge.org/core/terms. https://doi.org/10.1017/9780511609923.012

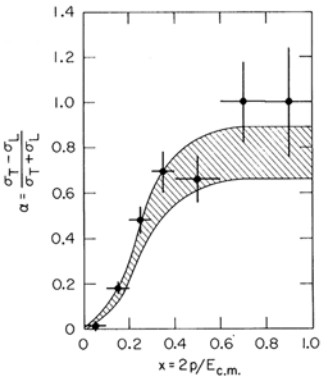


FIG. 4. Observed inclusive α versus x (from Ref. 9) for particles with $|\cos\theta| \leq 0.6$ in hadronic events at $E_{c.m.} = 7.4$ GeV. The prediction of the jet-model Monte Carlo simulation for jet-axis angular distribution with $\alpha = 0.78 \pm 0.12$ is represented by the shaded band.

4 values for the inclusive hadron α as a function of x at 7.4 GeV[9] are compared with the jet-model calculation. The model assumed the value $\alpha = 0.78 \pm 0.12$ for the jet-axis angular distribution. The prediction agrees well with the data for all values of x.

We conclude that the data strongly support the jet hypothesis for hadron production in e^+e^- annihilation. The data show a decreasing mean sphericity with increasing $E_{c.m.}$ and the sphericity distributions peak more strongly at low values as $E_{c.m.}$ increases. Both of these trends agree with a jet model and disagree with an isotropic PS model. The mean transverse momentum relative to the jet axis obtained using the jet-model Monte Carlo simulation was found to be 315 ± 2 MeV/c. At $E_{c.m.} = 7.4$ GeV the coefficient α for the jet-axis angular distribution in Eq. (4) has been found to be nearly $+1$ giving a value for σ_L/σ_T of 0.13 ± 0.07. The jet model also reproduces well the inclusive hadron α versus x. All of this indicates not only that there are jets but also that the helicity along the jet axis is ± 1. In the framework of the quark-parton model, the partons must must have spin $\frac{1}{2}$ rather than spin 0.

*Work supported by the U. S. Energy Research and Development Administration.

†Alfred P. Sloan Fellow.

‡Fellow of Deutsche Forschungsgemeinschaft.

§Permanent address: Centre d'Etudes Nucléaires de Saclay, Saclay, France

‖Permanent address: Institut de Physique Nucléaire, Orsay, France.

[1]S. D. Drell, D. J. Levy, and T. M. Yan, Phys. Rev. 187, 2159 (1969), and Phys. Rev. D 1, 1617 (1970).

[2]N. Cabibbo, G. Parisi, and M. Testa, Lett. Nuovo Cimento 4, 35 (1970).

[3]J. D. Bjorken and S. J. Brodsky, Phys. Rev. D 1, 1416 (1970).

[4]R. P. Feymann, *Photon-Hadron Interactions* (Benjamin, Reading, Mass., 1972), p. 166.

[5]J.-E. Augustin *et al.*, Phys. Rev. Lett. 34, 233 (1975).

[6]J.-E. Augustin *et al.*, Phys. Rev. Lett. 34, 764 (1975).

[7]It is impossible to determine the jet axis exactly, even with perfect detection efficiency; the method described here, which was suggested in Ref. 3, is the best approximation known to us.

[8]The momentum distributions will be discussed in a subsequent paper.

[9]R. F. Schwitters *et al.*, Phys. Rev. Lett. 35, 1320 (1975).

[10]Since the jet axis is a symmetry axis, the azimuthal angle $\varphi + 180°$ is equivalent to the azimuthal angle φ.

Downloaded from https://www.cambridge.org/core. UNIVERSIDAD AUTONOMA METROPOLITANA, on 19 Nov 2026 at 11:01:57, subject to the Cambridge Core terms of use, available at https://www.cambridge.org/core/terms. https://doi.org/10.1017/9780511609923.012

Volume 86B, number 2 PHYSICS LETTERS 24 September 1979

EVIDENCE FOR PLANAR EVENTS IN e^+e^- ANNIHILATION AT HIGH ENERGIES

TASSO Collaboration

R. BRANDELIK, W. BRAUNSCHWEIG, K. GATHER, V. KADANSKY, K. LÜBELSMEYER, P. MÄTTIG, H.-U. MARTYN, G. PEISE, J. RIMKUS, H.G. SANDER, D. SCHMITZ, A. SCHULTZ von DRATZIG, D. TRINES and W. WALLRAFF
I. Physikalisches Institut der RWTH Aachen, Germany [5]

H. BOERNER, H.M. FISCHER, H. HARTMANN, E. HILGER, W. HILLEN, G. KNOP, W. KORBACH, P. LEU, B. LÖHR, F. ROTH [1], W. RÜHMER, R. WEDEMEYER, N. WERMES and M. WOLLSTADT
Physikalisches Institut der Universität Bonn, Germany [5]

R. BÜHRING, R. FOHRMANN, D. HEYLAND, H. HULTSCHIG, P. JOOS, W. KOCH, U. KÖTZ, H. KOWALSKI, A. LADAGE, D. LÜKE, H.L. LYNCH, G. MIKENBERG [2], D. NOTZ, J. PYRLIK, R. RIETHMÜLLER, M. SCHLIWA, P. SÖDING, B.H. WIIK and G. WOLF
Deutsches Elektronen-Synchrotron DESY, Hamburg, Germany

M. HOLDER, G. POELZ, J. RINGEL, O. RÖMER, R. RÜSCH and P. SCHMÜSER
II. Institut für Experimentalphysik der Universität Hamburg, Germany [5]

D.M. BINNIE, P.J. DORNAN, N.A. DOWNIE, D.A. GARBUTT, W.G. JONES, S.L. LLOYD, D. PANDOULAS, A. PEVSNER [3], J. SEDGEBEER, S. YARKER and C. YOUNGMAN
Department of Physics, Imperial College, London, England [6]

R.J. BARLOW, R.J. CASHMORE, J. ILLINGWORTH, M. OGG and G.L. SALMON
Department of Nuclear Physics, Oxford University, England [6]

K.W. BELL, W. CHINOWSKY [4], B. FOSTER, J.C. HART, J. PROUDFOOT, D.R. QUARRIE, D.H. SAXON and P.L. WOODWORTH
Rutherford Laboratory, Chilton, England [6]

Y. EISENBERG, U. KARSHON, E. KOGAN, D. REVEL, E. RONAT and A. SHAPIRA
Weizmann Institute, Rehovot, Israel [7]

J. FREEMAN, P. LECOMTE, T. MEYER, SAU LAN WU and G. ZOBERNIG
Department of Physics, University of Wisconsin, Madison, WI, USA [8]

Received 29 August 1979

[1] Now at University Kiel, Germany. [2] On leave from Weizmann Institute, Rehovot, Israel. [3] On leave from Johns Hopkins University, Baltimore, MD, USA. [4] On leave from University of California, Berkeley, USA. [5] Supported by the Deutsches Bundesministerium für Forschung und Technologie. [6] Supported by the UK Science Research Council. [7] Supported by the Minerva Gesellschaft für die Forschung mbH, Munich, Germany. [8] Supported in part by the US Department of Energy, contract EY-76-C-02-0881.

Downloaded from https://www.cambridge.org/core. UNIVERSIDAD AUTONOMA METROPOLITANA, on 19 Nov 2026 at 11:01:57, subject to the Cambridge Core terms of use, available at https://www.cambridge.org/core/terms. https://doi.org/10.1017/9780511609923.012

Volume 86B, number 2 PHYSICS LETTERS 24 September 1979

Hadron jets produced in e^+e^- annihilation between 13 GeV and 31.6 GeV in c.m. at PETRA are analyzed. The transverse momentum of the jets is found to increase strongly with c.m. energy. The broadening of the jets is not uniform in azimuthal angle around the quark direction but tends to yield planar events with large and growing transverse momenta in the plane and smaller transverse momenta normal to the plane. The simple $q\bar{q}$ collinear jet picture is ruled out. The observation of planar events shows that there are three basic particles in the final state. Indeed, several events with three well-separated jets of hadrons are observed at the highest energies. This occurs naturally when the outgoing quark radiates a hard noncollinear gluon, i.e., $e^+e^- \to q\bar{q}g$ with the quarks and the gluons fragmenting into hadrons with limited transverse momenta.

It has been conjectured that hadron production in e^+e^- annihilation proceeds by quark pair production with the quarks fragmenting into two nearly collinear jets of hadrons [1–4]. The transverse momentum of the hadrons is limited at high energies such that narrow jets are predicted in the PETRA energy range. Data from SPEAR and DORIS support this picture [5,6]. In this paper we examine our data on e^+e^- annihilation at high energies for deviations from the simple quark parton picture [‡1]. Such deviations have been observed [8] in deep inelastic lepton scattering experiments and are expected [9] to occur in any field theory of strong interactions. Furthermore, final states observed [10] in the hadronic decay of the $\Upsilon(9.46)$ disagree with a naive $q\bar{q}$ picture.

This analysis is based on data collected at the DESY e^+e^- storage ring PETRA using the TASSO detector. A description of the experimental setup and of the data analysis has already been published [11]. We list here only the main points. The detector, which measures charged secondaries over approximately 87% of 4π, was triggered by demanding at least three tracks with a transverse momentum of more than 0.32 GeV/c with respect to the beam axis, at total energies $W = 2E_{\text{beam}} = 13$ and 17 GeV. At least four tracks were required at $W = 27.4$, 27.7, 30, and 31.6 GeV. The hadronic events were separated from the beam gas background by demanding that the event vertex was in the interaction volume, and that the sum of the detected momenta were above 3 GeV/c at 13 GeV energy, above 4 GeV/c at 17 GeV energy, and above 9 GeV/c at the higher energies. Further cuts on the event topology essentially eliminated $\gamma\gamma$ and $\tau^+\tau^-$ events. The resulting detection efficiency varied with energy between 75% and 78%. The final data sample consists of 75 events at 13 GeV, 40 events at 17 GeV, 118 events at 27.4 and 27.7 GeV, 135 events at 30 GeV, and 40 events at 31.6 GeV. For the following analysis only tracks that reached at least the sixth zero degree layer in the drift chamber ($|\cos\theta| < 0.87$) and had transverse momentum relative to the beam axis of at least 0.10 GeV/c, are used. Hadrons resulting from kaon decays were not removed while electrons from pair conversion or Dalitz decays were removed.

The effects of the selection criteria described above, as well as the effects of measuring errors and the efficiencies of the pattern recognition programs and the whole analysis chain, were checked by propagating Monte Carlo events through the simulated detector and the analysis programs. It was thus ascertained that the results presented in this paper are not subject to any significant bias due to these sources.

The quark parton picture of the process $e^+e^- \to q\bar{q}$ is depicted in fig. 1a. It will produce back-to-back jets of hadrons with typical transverse momenta of 0.30 GeV/c. In field theories of the strong interactions this picture will be modified [9,12] to include other processes including the lowest-order diagrams shown in fig. 1b. The radiated field quanta (gluons) are also expected to evolve into jets of hadrons. This has clear experimental implications [12–16]: The p_T distribution of the final hadrons will broaden with increasing energy. If the coupling constant is less than one there will be a tendency for only one of the jets to be broadened. The $q\bar{q}g$ state is necessarily planar; this should be reflected in the final hadron configuration which should retain the planarity with small transverse momenta with respect to the plane and large transverse momentum in the plane. If the gluon is radiated with a transverse momentum that is large compared to the typical transverse momentum of 0.30 GeV/c, then the event will have a three-jet topology [12].

Since in e^+e^- interactions the direction of the jet axis is not known from the initial state, it has to be

[‡1] Evidence for planar events in e^+e^- annihilation has been reported earlier, see ref. [7]. The present results are based on a five-fold increase of statistics.

Downloaded from https://www.cambridge.org/core. UNIVERSIDAD AUTONOMA METROPOLITANA, on 19 Nov 2026 at 11:01:57, subject to the Cambridge Core terms of use, available at https://www.cambridge.org/core/terms. https://doi.org/10.1017/9780511609923.012

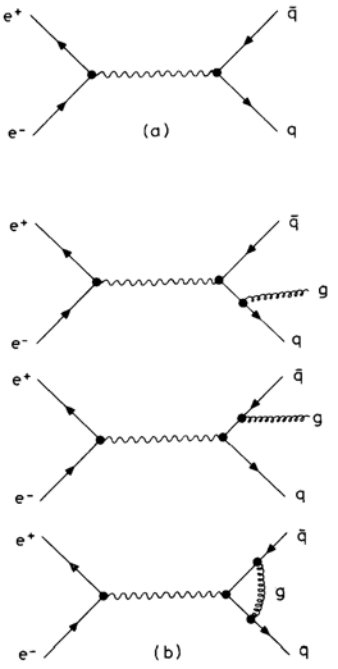


Fig. 1. Quark pair production and gluon bremsstrahlung to lowest order.

determined event by event from the final state hadrons. We have done this in two ways: Minimizing Σp_T^2 (which gives the sphericity axis) [3,5] or maximizing $\Sigma|p_\parallel|$ (which gives the thrust axis) [13,17]. The summations are over all observed hadrons. The results presented in this paper were generally found not to depend to any significant degree on the choice between these two possibilities [‡2]. Studies with Monte Carlo $q\bar{q}$ jets [18] [‡3] further showed that the jet axes so determined deviate by an average of less than 5° from the true jet axis at our higher energies.

The normalized transverse momentum distribution $\sigma^{-1}\, d\sigma/dp_T^2$ evaluated with respect to the sphericity axis is plotted in fig. 2 versus p_T^2. The data at 13 GeV and 17 GeV are identical within statistics and are averaged; similarly the higher energy data between 27.4 GeV and 31.6 GeV are combined. The data at both energies are in reasonable agreement for $p_T^2 < 0.2$ $(\mathrm{GeV}/c)^2$ but the high-energy data are well above the low-energy data for larger values of p_T^2. The average value of p_T^2 increases from 0.15 ± 0.02 $(\mathrm{GeV}/c)^2$ at 13 and 17 GeV, to 0.27 ± 0.02 $(\mathrm{GeV}/c)^2$ for the combined high-energy data. The low-energy data have been fitted for $p_T^2 < 1.0$ $(\mathrm{GeV}/c)^2$ with the jet model [18] [‡3] of Field and Feynman, extended to include c and b quarks [‡4]. In this model, the parameter σ_q determining the width of the p_T distribution was varied from the original value $\sigma_q = 0.25$ GeV/c to $\sigma_q = 0.30$ GeV/c to obtain a fit to our data. This is shown by the curve in fig. 2. To fit the higher-energy data with the Field–Feynman model, σ_q must be increased to 0.45 GeV/c. This is in contradiction to the naive quark parton model which assumes the quark to frag-

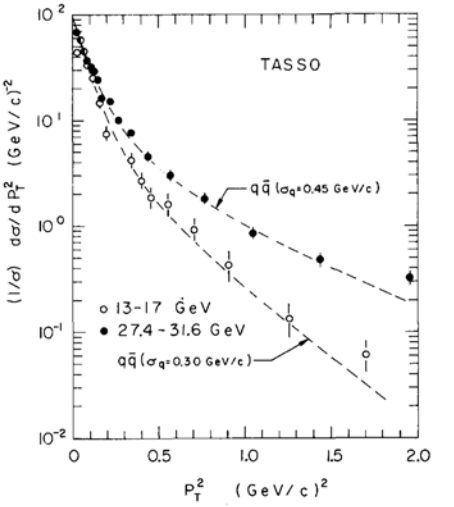


Fig. 2. $\sigma^{-1}\, d\sigma/dp_T^2$ at 13 and 17 GeV combined (○) and for 27.4 GeV, 27.7 GeV, 30.0 GeV and 31.6 GeV combined (•) as a function of p_T^2. The curves are fits to the data for $p_T^2 < 1.0$ GeV/c using the Field–Feynman quark–parton model including u, d, s, c and b quarks with σ_q as a free parameter.

‡2 An exception is the "seagull effect" shown in fig. 3. Here only the thrust axis is useful since the sphericity weights fast particles too heavily and thus biases the particles of high $z = p_h/p_{beam}$ towards small values of p_T.

‡3 For comparison with the data we used the version given by Field and Feynman [18].

‡4 The branching ratios for B meson decay were taken from ref. [19].

Downloaded from https://www.cambridge.org/core. UNIVERSIDAD AUTONOMA METROPOLITANA, on 19 Nov 2026 at 11:01:57, subject to the Cambridge Core terms of use, available at https://www.cambridge.org/core/terms. https://doi.org/10.1017/9780511609923.012

ment into hadrons with an energy-independent transverse momentum distribution. On the other hand, field theories of the strong interactions naturally predict the transverse momentum to increase with energy due to gluon bremsstrahlung by one of the outgoing quarks. The production of a new quark flavour will also lead to an increase in the average value of p_T. We do not find any evidence for the production of a new flavour in agreement [20] with other groups at PETRA.

If hard noncollinear gluon emission is a rare process, then there should usually be only one such gluon in these events. Dividing each event into two halves by a plane perpendicular to the jet axis and determining $\langle p_T^2 \rangle$ separately for the two sides, the "narrow" side should rarely have a noncollinear hard gluon. Thus $\langle p_T^2 \rangle_{\text{narrow}}$ will increase with energy less rapidly than $\langle p_T^2 \rangle_{\text{wide}}$. This is observed as shown in fig. 3 where $\langle p_T^2 \rangle$ is plotted as a function of $z = p/p_{\text{beam}}$ for the wide and the narrow jet separately. The $q\bar{q}$ model with $\sigma_q = 0.30$ GeV/c is also plotted in fig. 3a. It fits the data rather well at low energy; the narrow–wide asymmetry is due to statistical fluctuations. The model fails to describe the data at high energies (fig. 3b); however, increasing σ_q to 0.45 GeV/c, obtained from the fit to the p_T^2 distribution, approximately reproduces the observed z distribution. Therefore we can fit, within the statistical uncertainties, both the p_T^2 distributions and the seagull plot at both energies by increasing the value of σ_q with energy.

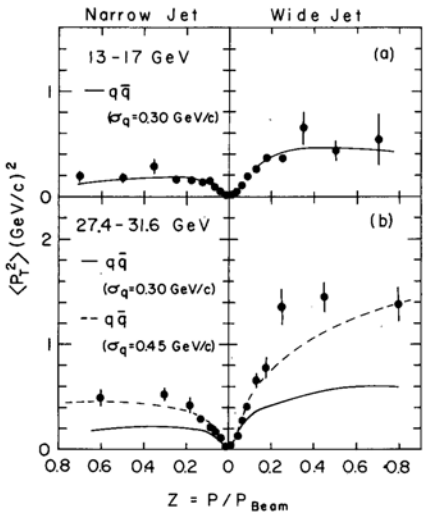


Fig. 3. $\langle p_T^2 \rangle$ as a function of $z = p/p_{\text{beam}}$ for the wide and narrow jet separately, for the low-energy (a) and the high-energy (b) data. The curves show the prediction from the $q\bar{q}$ model [18] [‡3] with $\sigma_q = 0.30$ GeV/c (solid curve) and $\sigma_q = 0.45$ GeV/c (dotted curve). The model includes u, d, s, c and b quarks.

Regardless of the value of $\langle p_T \rangle$ in the naive quark jet picture hadrons resulting from the fragmentation of the quark must be on the average uniformly distributed in azimuthal angle around the quark axis. Therefore, apart from statistical fluctuations, the two-jet process $e^+e^- \to q\bar{q}$ will not lead to planar events where as the radiation of a hard gluon, $e^+e^- \to q\bar{q}g$, will result in an approximately planar configuration of hadrons with large transverse momenta in the plane and small transverse momenta with respect to the plane. Thus the observation of such planar events at a rate significantly above the rate expected from statistical fluctuations of the $q\bar{q}$ jets shows in a model-independent way that there must be a third particle in the final state, which might be identified with a gluon.

The shape of the events is evaluated using the following method. For each event we construct the second-rank tensor [3,5] from the hadron momenta

$$M_{\alpha\beta} = \sum_{j=1}^{N} p_{j\alpha} p_{j\beta} \qquad (\alpha, \beta = x, y, z),$$

summing over all N observed charged particles. Let $\hat{n}_1$, $\hat{n}_2$ and $\hat{n}_3$ be the unit eigenvectors of this tensor associated with the smallest, intermediate, and largest eigenvalues Λ_1, Λ_2 and Λ_3, respectively. The principal jet axis is then the $\hat{n}_3$ direction, the event plane is the $\hat{n}_2$–$\hat{n}_3$ plane, and $\hat{n}_1$ defines the direction in which the sum of the squared hadron momenta components is minimized [21]. We compare in fig. 4 the distribution of

$$\langle p_T^2 \rangle_{\text{out}} = \frac{1}{N} \sum_{j=1}^{N} (p_j \cdot \hat{n}_1)^2$$

(the momentum component normal to the event plane squared) with that of

$$\langle p_T^2 \rangle_{\text{in}} = \frac{1}{N} \sum_{j=1}^{N} (p_j \cdot \hat{n}_2)^2$$

(the momentum component in the event plane per-

Downloaded from https://www.cambridge.org/core. UNIVERSIDAD AUTONOMA METROPOLITANA, on 19 Nov 2026 at 11:01:57, subject to the Cambridge Core terms of use, available at https://www.cambridge.org/core/terms. https://doi.org/10.1017/9780511609923.012

Volume 86B, number 2 PHYSICS LETTERS 24 September 1979

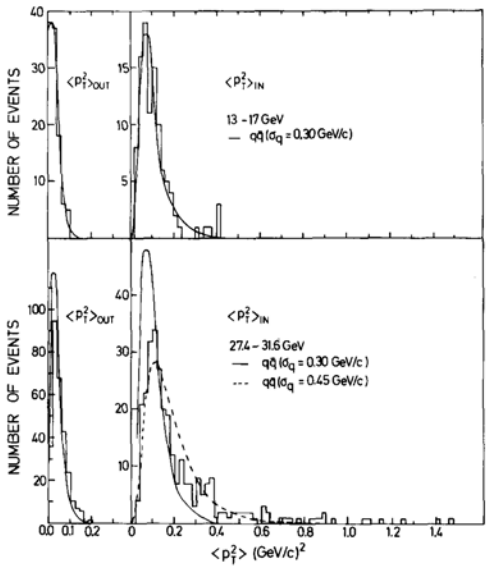


Fig. 4. The mean transverse momentum squared normal to the event plane $\langle p_T^2 \rangle_{out}$ and in the event plane $\langle p_T^2 \rangle_{in}$ per event for the low-energy and the high-energy data. The predictions from the quark model [18] ‡3 are shown assuming σ_q = 0.30 GeV/c (solid curves) and σ_q = 0.45 GeV/c (dotted curve). The model includes u, d, s, c and b quarks.

pendicular to the jet axis). The data show only little increase in $\langle p_T^2 \rangle_{out}$ between the low-energy and the high-energy point. The distribution of $\langle p_T^2 \rangle_{in}$, however, becomes much wider at high energies, and in particular there is a long tail of events with a large value of $\langle p_T^2 \rangle_{in}$ not observed at lower energies. The curves show the expectations from the Monte Carlo $q\bar{q}$ jets. Hadrons resulting from pure $q\bar{q}$ events will on the average be distributed uniformly around the jet axis, however, some asymmetry between $\langle p_T^2 \rangle_{in}$ and $\langle p_T^2 \rangle_{out}$ is caused by statistical fluctuations. Fair agreement with the $q\bar{q}$ model is found both for $\langle p_T^2 \rangle_{in}$ and $\langle p_T^2 \rangle_{out}$ at the low-energy point. Thus the asymmetry observed at this energy can be explained by statistical fluctuations only.

At the high energy, we find fair agreement between $\langle p_T^2 \rangle_{out}$ and the $q\bar{q}$ model with σ_q = 0.30 GeV/c, however, the observed long tail of the $\langle p_T^2 \rangle_{in}$ distribution is not reproduced by the model. This discrepancy cannot be removed by increasing the mean transverse momentum of the $q\bar{q}$ jets. The result from the model with σ_q = 0.45 GeV/c is also plotted in fig. 4. The agreement is poor. We therefore conclude that the data include a number of planar events not reproduced by the $q\bar{q}$ model, independent of the assumption on the average p_T in that model.

The normalized eigenvalues,

$$Q_k = \Lambda_k \Big/ \sum_{j=1}^{N} p_j^2 ,$$

may be used for a more detailed study of the shape of the events. These normalized eigenvalues Q_k satisfy $Q_1 + Q_2 + Q_3 = 1$ and are arranged such that $0 \leqslant Q_1 \leqslant Q_2 \leqslant Q_3$. We express our data in terms of two variables, aplanarity A and sphericity S:

$$A = \tfrac{3}{2} Q_1 = \tfrac{3}{2} \langle p_T^2 \rangle_{out} / \langle p^2 \rangle ,$$

$$S = \tfrac{3}{2} (Q_1 + Q_2) = \tfrac{3}{2} \langle p_T^2 \rangle / \langle p^2 \rangle .$$

All the events are then inside a triangle shown in fig. 5, where S is the hypotenuse of the triangle. The event distribution in A and S is shown in fig. 5, for the low-energy and high-energy data separately.

Collinear two-jet events lie in the left-hand corner

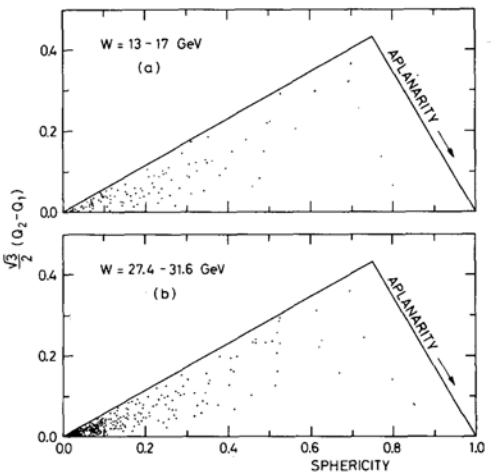


Fig. 5. Distribution of the events as a function of aplanarity $A = \frac{3}{2} Q_1 = \frac{3}{2} \langle p_T^2 \rangle_{out} / \langle p^2 \rangle$ and sphericity $S = \frac{3}{2} (Q_1 + Q_2) = \frac{3}{2} \langle p_T^2 \rangle / \langle p^2 \rangle$ for the low (a) and high (b) energy data.

Downloaded from https://www.cambridge.org/core. UNIVERSIDAD AUTONOMA METROPOLITANA, on 19 Nov 2026 at 11:01:57, subject to the Cambridge Core terms of use, available at https://www.cambridge.org/core/terms. https://doi.org/10.1017/9780511609923.012

(A, S small), uniform disk shaped events in the upper corner (A small, S large), and spherical events in the lower right-hand corner (A, S large), while coplanar events will occupy a band along the larger of the two small sides of the triangle in fig. 5.

Collinear two-jet events are seen to dominate at all energies, the collinearity being most pronounced at the highest energy. We exclude these events and select the candidates for planar events by requiring that $A < 0.04$ and $S > 0.25$. At 13 and 17 GeV we observe six events in this region compared to 3.5 events predicted by the $q\bar{q}$ model with $\sigma_q = 0.30$ GeV/c. At the higher energies we find 18 events compared to 4.5 events predicted by the $q\bar{q}$ model, independent of σ_q between 0.30 and 0.45 GeV/c. As an independent test of the planar structure, a randomization procedure [‡5] was applied to the data to destroy any natural correlations. This estimate of accidentally planar events yields six events in the 13–17 GeV data and four events in the higher-energy data. Thus at the higher energies there is an excess of planar events well above the level predicted from statistical fluctuations of the $q\bar{q}$ jets. This shows that $e^+e^- \to$ hadrons proceeds via the creation and decay of at least three primary particles that subsequently fragment into hadrons. Field theories of the strong interactions predict such a topology resulting from the radiation of a field quantum (gluon) by one of the quarks, i.e., $e^+e^- \to q\bar{q}g$.

If this is the correct explanation and the gluon materializes as a jet of hadrons with limited transverse momentum then a small fraction of the events should display a three-jet structure. The events were analyzed for a three-jet structure as described in ref. [21]. All the coplanar events gave a good fit to the three-jet hypothesis. We further determined the transverse momenta of the hadrons with respect to the axis to which they were assigned. For the 18 events defined above we find an average transverse momentum of about 0.30 GeV/c, close to the mean p_T observed in two-jet events at lower energies.

To compare this new class of three-jet events with the predominant class of two-jet events, fig. 6 shows a characteristic event of each type in momentum space in all three projections. Figs. 6a and 6d show a two-jet and a three-jet event, respectively, in the $\hat{n}_2$–$\hat{n}_3$ plane; this is the plane containing the largest components of momenta. The first event shows two clearly delineated jets. The three-jet event, on the other hand, shows a much broader distribution of momenta transverse to the $\hat{n}_3$ axis. Figs. 6b and 6e show the projection on the plane perpendicular to the jet direction ($\hat{n}_3$). Here one clearly sees the small transverse momenta for the two-jet event and the tendency of the large transverse momentum to lie along the $\hat{n}_2$ direction for the three-jet event. Finally figs. 6c and 6f show the remaining projection on the $\hat{n}_1$–$\hat{n}_3$ plane.

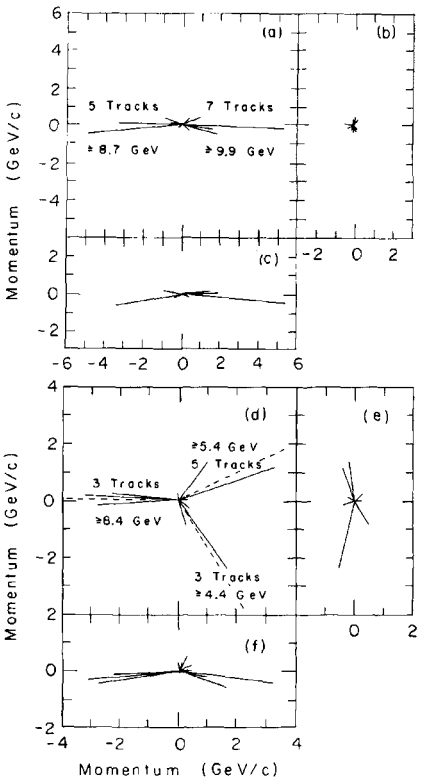


Fig. 6. Momentum space representation of a two-jet event (a)–(c) and a three-jet event (d)–(f) in each of three projections. (a), (d) $\hat{n}_2$–$\hat{n}_3$ plane; (b), (e) $\hat{n}_1$–$\hat{n}_2$ plane; (c), (f) $\hat{n}_1$–$\hat{n}_3$ plane.

[‡5] The sphericity axis was chosen as a reference, and all tracks were rotated by a random azimuthal angle around the jet direction; this preserves both p_T and $p_\parallel$. Then at random the sign of $p_\parallel$ was changed.

Downloaded from https://www.cambridge.org/core. UNIVERSIDAD AUTONOMA METROPOLITANA, on 19 Nov 2026 at 11:01:57, subject to the Cambridge Core terms of use, available at https://www.cambridge.org/core/terms. https://doi.org/10.1017/9780511609923.012

In summary, we have studied $e^+e^- \to$ hadrons for values of Q^2 between 170 $(GeV/c)^2$ and 1000 $(GeV/c)^2$. We observe a change in the p_T^2 distribution and a strong increase of $\langle p_T^2 \rangle$ with increasing energy. This increase occurs predominantly in only one of the two jets. The distribution of the transverse momentum perpendicular to the "event plane" does not show a pronounced energy dependence while a strong broadening takes place in the event plane at the highest values of Q^2. We observe planar events at a rate which is well above the rate computed for statistical fluctuations of the $q\bar{q}$ jets. The planar events exhibit three axes, the average transverse momentum of the hadrons with respect to these axes being 0.30 GeV/c. This establishes in a model-independent way that a small fraction of the e^+e^- annihilation events proceeds via maemission of three primary particles, each of which materializes as a jet of hadrons in the final state. The data are most naturally explained by hard noncollinear bremsstrahlung $e^+e^- \to q\bar{q}g$. Indeed, the data are in agreement with predictions based on first-order perturbative QCD as will be discussed in a forthcoming paper.

We thank the DESY directorate for its strong support of this experiment. We are grateful for the diligent efforts of the PETRA machine group which made this experiment possible. We are indebted to all the engineers and technicians of the collaborating institutions who have participated in the construction and maintenance of TASSO. The excellent cooperation with the technical support groups at DESY and at the Rutherford Lab. is gratefully acknowledged. The Wisconsin group thanks the Physics Department of the University of Wisconsin for support, especially the High Energy Group and the Graduate School Research Committee.

References

[1] S.D. Drell, D.J. Levy and T.M. Yan, Phys. Rev. 187 (1969) 2159; D1 (1970) 1617.
[2] N. Cabibbo, G. Parisi and M. Testa, Lett. Nuovo Cimento 4 (1970) 35.
[3] J.D. Bjorken and S.J. Brodsky, Phys. Rev. D1 (1970) 1416.
[4] R.P. Feynman, Photon–hadron interactions (Benjamin, Reading, MA, 1972) p. 166.
[5] G. Hanson et al., Phys. Rev. Lett. 35 (1975) 1609.
[6] Ch. Berger et al., Phys. Lett. 78B (1978) 176.
[7] B.H. Wiik, Proc. Intern. Neutrino Conf. (Bergen, Norway, 18–22 June 1979);
R. Cashmore, P. Söding and G. Wolf, Proc. EPS Intern. Conf. on High energy physics (Geneva, Switzerland, 27 June–4 July 1979).
[8] E.M. Riordan et al., SLAC preprint PUB-1639 (1975);
D.J. Fox et al., Phys. Rev. Lett. 37 (1974) 1504;
H.L. Anderson et al., Phys. Rev. Lett. 37 (1976) 4;
P.C. Bosetti et al., Nucl. Phys. B142 (1978) 1;
J.G.H. de Groot et al., Particles and Fields (Z. Phys. C) 1 (1979) 143; Phys. Lett. 82B (1979) 292, 456.
[9] J. Kogut and L. Susskind, Phys. Rev. D9 (1974) 697, 3391;
A.M. Polyakov, Proc. 1975 Intern. Symp. on Lepton and photon interactions at high energies (Stanford), ed. W.T. Kirk (SLAC, Stanford, 1975) p. 855.
[10] PLUTO Collaboration, Ch. Berger et al., Phys. Lett. 82B (1979) 449;
S. Brandt, Paper presented at the Intern. Conf. on High energy physics (Geneva, 27 June–4 July 1979).
[11] TASSO Collaboration, R. Brandelik et al., Phys. Lett. 83B (1979) 201.
[12] J. Ellis, M.K. Gaillard and G.G. Ross, Nucl. Phys. B111 (1976) 253; Erratum B130 (1977) 516.
[13] A. de Rujula, J. Ellis, E.G. Floratos and M.K. Gaillard, Nucl. Phys. B138 (1978) 387.
[14] T.A. DeGrand, Yee Jack Ng and S.-H.H. Tye, Phys. Rev. D16 (1977) 3251.
[15] P. Hoyer, P. Osland, H.G. Sander, T.F. Walsh and P.M. Zerwas, DESY 78/21, to be published.
[16] G. Kramer and G. Schierholz, Phys. Lett. 82B (1979) 102;
G. Kramer, G. Schierholz and J. Willrodt, Phys. Lett. 79B (1978) 249;
G. Curci, M. Greco and Y. Srivastava, CERN-Report 2632-1979.
[17] E. Fahri, Phys. Rev. Lett. 39 (1977) 1587;
S. Brandt and H.D. Dahmen, Particles and Fields (Z. Phys. C) 1 (1979) 61.
[18] B. Anderson, G. Gustafson and C. Peterson, Nucl. Phys. B135 (1978) 273;
R.D. Field and R.P. Feynman, Nucl. Phys. B136 (1978) 1;
[19] A. Ali, J.G. Körner, J. Willrodt and G. Kramer, Particles and Fields (Z. Phys. C) 1 (1979) 269; 2 (1979) 33.
[20] See papers contributed by the JADE, MARK J, PLUTO and TASSO Collaborations to the 1979 Intern. Symp. on Lepton and photon interactions at high energies (Batavia, IL, USA, August 23–29, 1979).
[21] S.L. Wu and G. Zobernig, Particles and Fields (Z. Phys. C) 2 (1979) 107.

Downloaded from https://www.cambridge.org/core. UNIVERSIDAD AUTONOMA METROPOLITANA, on 19 Nov 2026 at 11:01:57, subject to the Cambridge Core terms of use, available at https://www.cambridge.org/core/terms. https://doi.org/10.1017/9780511609923.012

Volume 118B, number 1, 2, 3 PHYSICS LETTERS 2 December 1982

OBSERVATION OF VERY LARGE TRANSVERSE MOMENTUM JETS AT THE CERN $\bar{p}p$ COLLIDER

The UA2 Collaboration

M. BANNER [f], Ph. BLOCH [f], F. BONAUDI [b], K. BORER [a], M. BORGHINI [b], J.-C. CHOLLET [d], A.G. CLARK [b], C. CONTA [e], P. DARRIULAT [b], L. Di LELLA [b], J. DINES-HANSEN [c], P.-A. DORSAZ [b], L. FAYARD [d], M. FRATERNALI [e], D. FROIDEVAUX [b,d], J.-M. GAILLARD [d], O. GILDEMEISTER [b], V.G. GOGGI [e,1], H. GROTE [b], B. HAHN [a], H. HÄNNI [a], J.R. HANSEN [b], P. HANSEN [c], T. HIMEL [b], V. HUNGERBÜHLER [b], P. JENNI [b], O. KOFOED-HANSEN [c], M. LIVAN [e], S. LOUCATOS [f], B. MADSEN [c], B. MANSOULIÉ [f], G.C. MANTOVANI [e,2], L. MAPELLI [b], B. MERKEL [d], M. MERMIKIDES [b], R. MØLLERUD [c], B. NILSSON [c], C. ONIONS [b], G. PARROUR [b,d], F. PASTORE [b], H. PLOTHOW-BESCH [d], J.-P. REPELLIN [d], J. RINGEL [b], A. ROTHENBERG [b], A. ROUSSARIE [f], G. SAUVAGE [d], J. SCHACHER [a], J.L. SIEGRIST [b], F. STOCKER [a], J. TEIGER [f], V. VERCESI [e], H.H. WILLIAMS [b], H. ZACCONE [f] and W. ZELLER [a]

[a] *Laboratorium für Hochenergiephysik, Universität Bern, Sidlerstrasse 5, Bern, Switzerland*
[b] *CERN, 1211 Geneva 23, Switzerland*
[c] *Niels Bohr Institute, Blegdamsvej 17, Copenhagen, Denmark*
[d] *Laboratoire de l'Accélérateur Linéaire, Université de Paris-Sud, Orsay, France*
[e] *Istituto di Fisica Nucleare, Università di Pavia and INFN, Sezione di Pavia, Via Bassi 6, Pavia, Italy*
[f] *Centre d'Etudes Nucléaires de Saclay, Gif sur Yvette, France*

Received 25 August 1982

The distribution of total transverse energy ΣE_T over the pseudorapidity interval $-1 < \eta < 1$ and an azimuthal range $\Delta\phi = 300°$ has been measured in the UA2 experiment at the CERN $\bar{p}p$ collider ($\sqrt{s} = 540$ GeV) using a highly segmented total absorption calorimeter. In the events with very large ΣE_T ($\Sigma E_T \gtrsim 60$ GeV) most of the transverse energy is found to be contained in small angular regions as expected for high transverse momentum hadron jets. We discuss the properties of a sample of two-jet events with invariant two-jet masses up to 140 GeV/c^2 and we measure the cross section for inclusive jet production in the range of jet transverse momenta between 15 and 60 GeV/c.

1. Introduction. The suggestion that hard scattering of hadron constituents should result in two jets with the same momenta as the scattered partons [1] has motivated an intense experimental effort [2]. Earlier ISR experiments [3] have reported observations of such double-jet structures. However these jets were not as clearly identified as they are in the hadronic final states of high-energy e^+e^- annihilations [4], because in hadronic collisions the jets carry only a fraction of the total energy available. As a consequence, jets are accompanied by several soft hadrons which may make their identification more difficult and in general they are not collinear.

The recent successful operation of the CERN $\bar{p}p$ collider [5] has opened a new possibility to observe high transverse momentum hadron jets. At $\sqrt{s} = 540$ GeV the yield of jets with $E_T > 20$ GeV is expected to increase by about four orders of magnitude with respect to the top ISR energy [6] whereas the average particle density in the central region for an ordinary collision has increased by less than a factor of 2 [7].

We report here on results from the UA2 experiment at the CERN $\bar{p}p$ collider. This experiment uses a large

[1] Now also at Istituto di Fisica, Università di Udine, Italy.
[2] Now also at Istituto di Fisica, Università di Perugia, Italy.

0 031-9163/82/0000–0000/$02.75 © 1982 North-Holland

Downloaded from https://www.cambridge.org/core. UNIVERSIDAD AUTONOMA METROPOLITANA, on 19 Nov 2026 at 11:01:57, subject to the Cambridge Core terms of use, available at https://www.cambridge.org/core/terms. https://doi.org/10.1017/9780511609923.012

Volume 118B, number 1, 2, 3 PHYSICS LETTERS 2 December 1982

solid angle total absorption hadron calorimeter subdivided in small cells, a device well suited to the detection of hadron jets.

2. Apparatus. A cross section of the UA2 detector is shown in fig. 1. At the centre of the apparatus a vertex detector consisting of cylindrical proportional and drift chambers measures particle trajectories in a region without magnetic field.

The vertex detector is surrounded by a highly segmented electromagnetic and hadronic calorimeter (the central calorimeter) which covers the pseudorapidity interval $-1 < \eta < 1$ (polar angle $40° < \theta < 140°$) and an azimuthal range of 300°. In the present stage of the experiment the remaining azimuthal interval (±30° around the horizontal plane) is covered by a single arm spectrometer to measure charged and neutral particle production [8].

The forward and backward regions ($20° < \theta < 37.5°$ and $142.5° < \theta < 160°$, respectively), are each instrumented by twelve toroidal magnet sectors followed by drift chambers, multitube proportional chambers and electromagnetic calorimeters.

The central calorimeter is segmented into 200 cells, each covering 15° in ϕ and 10° in θ and built in a tower structure pointing to the centre of the interaction region. The cells are segmented longitudinally into a 17 radiation length thick electromagnetic compartment (lead-scintillator) followed by two hadronic compartments (iron-scintillator) of two absorption lengths each. The light from each compartment is collected by two BBQ-doped light guide plates on opposite sides of the cell.

All calorimeters, including the forward–backward modules, have been calibrated in a 10 GeV/c beam from the CERN PS using incident electrons and muons. The calibration has since been tracked with a Xe light flasher system. In addition, the response of the electromagnetic compartments is checked regularly by accurately positioning a Co^{60} source in front of each cell and measuring the direct current from each photomultiplier. The systematic uncertainty in the energy calibration for the data discussed here is less than ±2% for the electromagnetic calorimeter and less than ±3% for the hadronic one.

The response of the calorimeter to electrons, single hadrons and multi-hadrons (produced in a target located in front of the calorimeter) has been measured at the CERN PS and SPS machines using beams from 1 to 70 GeV. In particular, we have studied the longi-

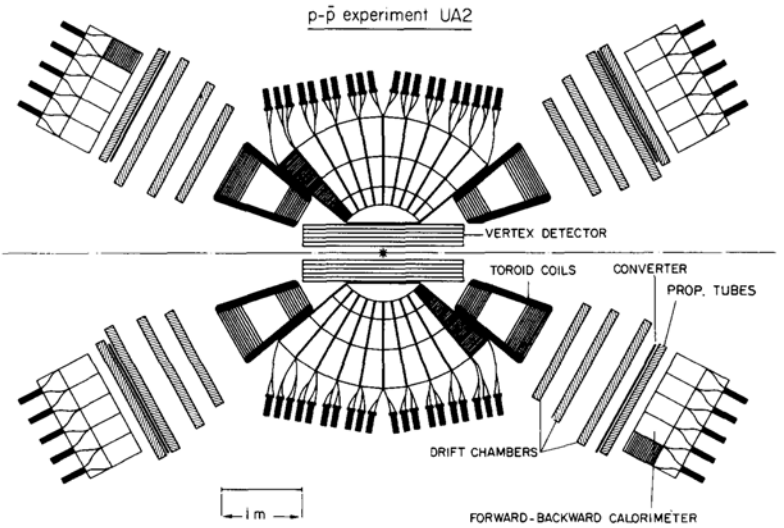


Fig. 1. The UA2 detector: schematic cross section in the vertical plane containing the beam.

Downloaded from https://www.cambridge.org/core. UNIVERSIDAD AUTONOMA METROPOLITANA, on 19 Nov 2026 at 11:01:57, subject to the Cambridge Core terms of use, available at https://www.cambridge.org/core/terms. https://doi.org/10.1017/9780511609923.012

tudinal and transverse shower development and the effect of particles impinging near the cell boundaries.

The energy resolution for electrons is measured to be $\sigma_E/E = 0.14/\sqrt{E}$ (E in GeV). In the case of hadrons, σ_E/E varies from 32% at 1 GeV to 11% at 70 GeV. The resolution for multi-hadron systems of more than 20 GeV is similar to that of single hadrons.

Details of the construction and performance of the calorimeter are reported elsewhere [9].

3. Data taking. The data discussed in this paper were recorded using a trigger sensitive to events with large transverse energy in the central calorimeter [10]. The gains of the photomultipliers were adjusted so that their signals were proportional to transverse energy. The signals were linearly added and their sum was required to exceed a given threshold (typically set at 20 GeV).

In order to suppress background from sources other than $\bar{p}p$ collisions, we required a coincidence with two additional signals obtained from two scintillator arrays surrounding the vacuum chamber 10.3 metres downstream of the interaction point and covering an interval $\Delta\eta = 1.1$ around $\eta = \pm 4.7$.

A sample of "minimum bias" data was recorded simultaneously by using only the coincidence of the signals from the two scintillator arrays. The rate of such coincidences provided also a measurement of the luminosity [8].

Furthermore the electronics were enabled between $\bar{p}p$ crossings and the cosmic ray background was found to be negligible.

4. Data reduction. Data have been recorded for an integrated luminosity of 79 μb^{-1}. The full data sample has been used in the following analysis for $\Sigma E_T > 30$ GeV. Partial samples are used for $\Sigma E_T < 30$ GeV and for minimum bias events.

The background events from beam halo particles and the accidental overlap of beam halo particles with minimum bias events exhibit a characteristic pattern in the detector different from that for events from $\bar{p}p$ collisions. A series of selection criteria is applied to remove background events:

– A fast filter requires that the pattern of hits in the vertex detector be consistent with charged particles coming from a common vertex.

– The ratios of the energies in each calorimeter layer (electromagnetic, first and second hadronic) to the total observed energy must be physically sensible.

– The local patterns of energy deposition in depth in the central calorimeter have to be consistent with that expected for particles emerging from a $\bar{p}p$ collision.

– Finally, for the highest ΣE_T events we reconstruct the event vertex and verify that it is within the collision region.

The combination of these requirements reduces strongly the number of background events. We find that the ratio of signal to background triggers in the initial event sample is ΣE_T-dependent, varying from $\sim$10 at $\Sigma E_T \lesssim 10$ GeV to $\sim$1 at 30 GeV and $\sim$0.25 at $\Sigma E_T > 60$ GeV. After applying all of the above cuts we estimate from a visual scan of events that the final event sample contains less than 10% of background events independently of ΣE_T.

To study the loss of good events introduced by the cuts described above we use test beam data, Monte Carlo simulations and we investigate the effect of varying the cuts on the data. We estimate that the loss of good events is $\lesssim$15%, independent of ΣE_T.

5. Transverse energy distribution. The total hadronic energy in a cell is measured as the sum of the energies in the three compartments (at least one compartment must have 150 MeV, well above pedestal fluctuations).

The distribution of events as a function of the transverse energy ΣE_T in the interval $-1 < \eta < +1$, $30° < \phi < 330°$ is presented in fig. 2a; it is observed to fall off exponentially as has been observed in experiments [11] with a similar solid angle coverage at the SPS nd at Fermilab ($\sqrt{s} = 24$ GeV). There are 10 events having $\Sigma E_T > 60$ GeV.

We estimate that the uncertainty in the energy scale due to systematic effects (150 MeV minimum cell energy, variation in response of the electromagnetic compartment for charged and neutral pions, and calibration errors [‡1] to be ±5%. In the lower energy experiments, events with large ΣE_T (the largest accessible value is approximately 20 GeV) have predominantly high multiplicity, cylindrically symmetrical

[‡1] The response to hadrons has been measured to be linear to within 2% over the whole energy range, that of the electromagnetic compartment differs by 17% between charged and neutral pions.

Downloaded from https://www.cambridge.org/core. UNIVERSIDAD AUTONOMA METROPOLITANA, on 19 Nov 2026 at 11:01:57, subject to the Cambridge Core terms of use, available at https://www.cambridge.org/core/terms. https://doi.org/10.1017/9780511609923.012

Volume 118B, number 1, 2, 3 PHYSICS LETTERS 2 December 1982

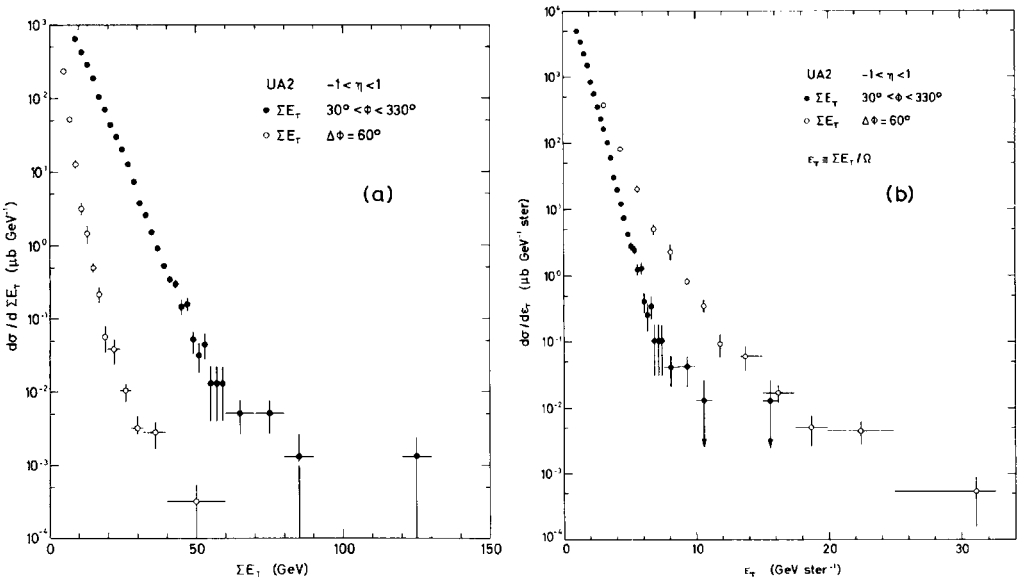


Fig. 2. Transverse energy (a) and its average density (b): observed distributions over the whole azimuthal acceptance (full dots) and over a restricted azimuthal region, $\Delta\phi = 60°$ (open circles).

configurations. It is however commonly expected [12] that at the present collider energy, $\sqrt{s} = 540$ GeV, sufficiently large values of ΣE_T can be reached that two-jet configurations resulting from hard scattering will dominate. An indication of this is already provided by the fact that the two highest energy points in fig. 2a lie significantly above the exponential.

A more sensitive test is provided by studying the ΣE_T distribution into a solid angle which is substantially smaller though still sufficiently large to contain most of the energy for hadron jets in the E_T region of interest ($E_T > 15$ GeV). The $d\sigma/d\Sigma E_T$ distribution for $-1 < \eta < 1$, $\Delta\phi = 60°$ is shown in fig. 2a; it demonstrates a clear departure from an exponential. In fig. 2b, the same data samples are plotted as a function of the transverse energy density, $\epsilon_T = \Sigma E_T/\Delta\Omega$. Figs. 2a,b illustrate that regions of high energy density are confined to within a small solid angle.

Direct evidence for an increase of the energy clustering towards higher values of ΣE_T is obtained by constructing clusters of adjacent cells, each cell containing more than a fraction f of the total energy deposited in the central calorimeter. When ΣE_T increases from 30 to >60 GeV, the number of such clusters decreases from ≃15 to ≃6 on the average for $f = 1\%$, while it increases from ≃0.7 to ≃2 for $f = 8\%$: events with a high value of ΣE_T are made of relatively less numerous but more energetic clusters.

The same fact is illustrated by determining for each event the two non-overlapping 45° × 40° solid angles which together contain the largest fraction, g, of the total transverse energy, and studying g as a function of ΣE_T; the average value of g increases from ≃40% at $\Sigma E_T = 30$ GeV to ≃60% for $\Sigma E_T > 60$ GeV.

To study these high ΣE_T events in detail we use a clustering algorithm which joins into a cluster all cells which share a common side and contain an energy $E_{cell} > E_{cell}^{min}$; E_{cell}^{min} is normally chosen to be 400 MeV, though the results obtained are relatively insensitive to the exact value chosen. Clusters having two or more local maxima separated by a valley deeper than 2 GeV are then split. On the average, for $\Sigma E_T > 30$ GeV, we obtain ≃4.4 clusters having $E_T > 2$ GeV per event, each cluster consisting of typically 4 cells.

The cluster (resp. the two clusters) with the largest transverse energy in an event accounts for a fraction

Downloaded from https://www.cambridge.org/core. UNIVERSIDAD AUTONOMA METROPOLITANA, on 19 Nov 2026 at 11:01:57, subject to the Cambridge Core terms of use, available at https://www.cambridge.org/core/terms. https://doi.org/10.1017/9780511609923.012

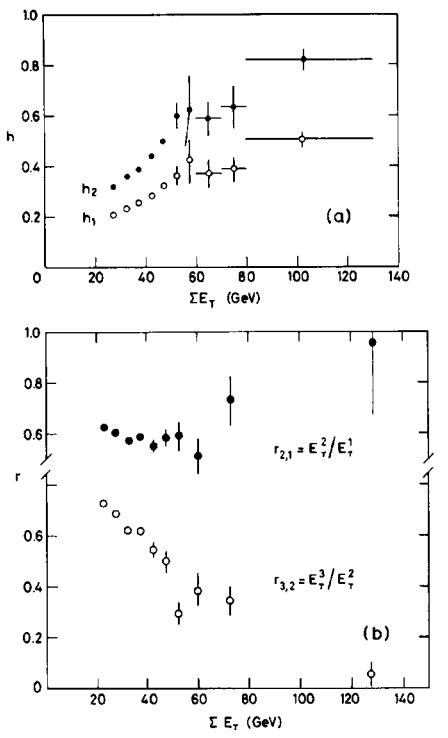


Fig. 3. (a) The fractions h_1 and h_2 of the total transverse energy ΣE_T contained in the cluster, and respectively the two clusters, having the largest E_T are displayed versus ΣE_T. (b) Dependence upon ΣE_T of the ratios $r_{21} = E_T^2/E_T^1$ and $r_{32} = E_T^3/E_T^2$ (see text).

h_1 (resp. h_2) of the total transverse energy ΣE_T measured in the central calorimeter. The dependence upon ΣE_T of h_1 and h_2 is illustrated in fig. 3a. In particular all events with ΣE_T in excess of 60 GeV have an average of 67% of the transverse energy contained in only two clusters.

6. Two-jet events. Fig. 4 shows the configuration of the event with the largest value of ΣE_T, 127 GeV. It exhibits striking features: energy is concentrated within two small regions separated in azimuth by $\Delta\phi \simeq 180°$ and towards which several collimated tracks are observed to point. In addition the transverse energies of the two clusters are approximately equal (57 and 60 GeV).

We now investigate to which extent such characteristics are also present in the other events having a large value of ΣE_T.

In each event we rank the central calorimeter clusters (C1, C2, ...) in order of decreasing transverse energies ($E_T^1 > E_T^2 > ...$). Fig. 5a shows the azimuthal separation $\Delta\phi$ between C1 and C2 for $E_T^{1,2} > 10$ GeV and $E_T^{1,2} > 14$ GeV. It peaks strongly near $\Delta\phi \simeq 180°$. If however we release the constraint that both E_T^1 and E_T^2 must exceed a high threshold, we find events in which E_T^2 may be only a small fraction of E_T^1: for example, in the sample of 59 events having $E_T^1 > 20$ GeV, 41 have $E_T^2/E_T^1 < 0.4$. For those $\Delta\phi$ is observed to have a uniform distribution between 0 and 180° while it always exceeds 140° in the rest of the sample. It is then natural to consider the possibility that a large localised transverse energy be produced outside the central calorimeter acceptance. Indeed, of 385 events having $E_T^1 > 10$ GeV and $E_T^2/E_T^1 < 0.4$, 22 deposit more than 5 GeV transverse energy in a sector of one of the forward/backward electromagnetic calorimeters: in such cases the azimuthal separation $\Delta\phi$ between this sector and C1 is nearing 180° (fig. 5b). These observations suggest an interpretation of the events in terms of a hard parton collision, a characteristic feature of which is the coplanarity of the scattered partons with the incident beams.

Further evidence is obtained from the fact that C1 and C2 are associated with jets of particles. We select a sample S_{JJ} (55 events) by requiring $E_T^{1,2} > 10$ GeV and $\Delta\phi > 140°$. We make the following observations:

(i) several tracks, measured in the vertex detector, are observed to aim towards the cluster centers (to within 13° on the average for $E_T > 20$ GeV);

(ii) longitudinal shower developments, measured from the contributions of electromagnetic and hadronic compartments, are inconsistent with that of a single particle but consistent with that of a jet fragmenting into charged and neutral pions;

(iii) cluster diameters are ≈80% larger than expected from the transverse extension of showers induced by single particles but are consistent with fragmenting jets.

We use the same event sample S_{JJ} to investigate a third property of hard parton collisions: the approximate equality of the transverse momenta of the scattered partons. We calculate the transverse momentum P_T and the invariant mass M associated with the pair

Downloaded from https://www.cambridge.org/core. UNIVERSIDAD AUTONOMA METROPOLITANA, on 19 Nov 2026 at 11:01:57, subject to the Cambridge Core terms of use, available at https://www.cambridge.org/core/terms. https://doi.org/10.1017/9780511609923.012

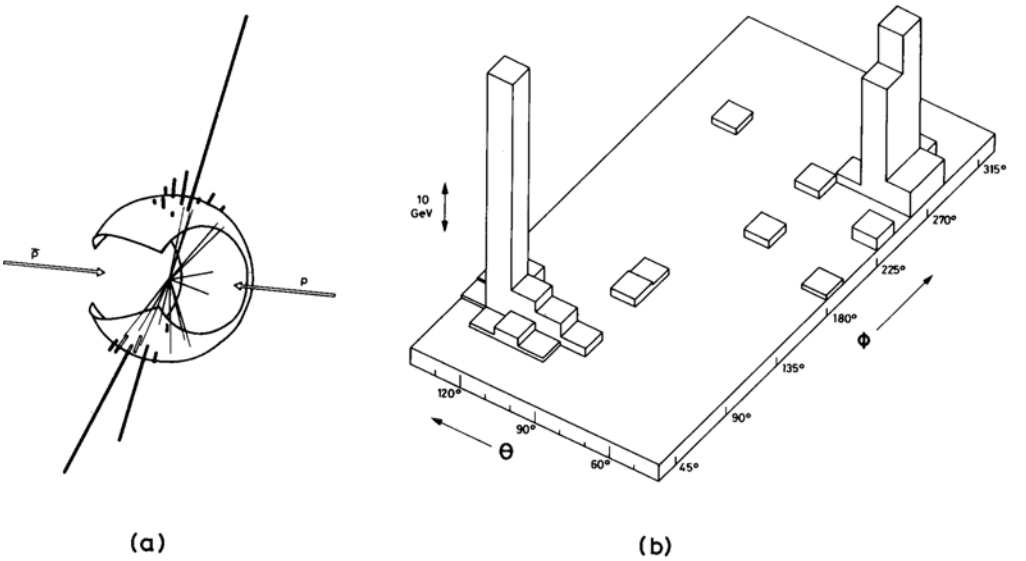


Fig. 4. Configuration of the event with the largest value of ΣE_T, 127 GeV (M = 140 GeV): (a) charged tracks pointing to the inner face of the central calorimeter are shown together with cell energies (indicated by heavy lines with lengths proportional to cell energies). (b) the cell energy distribution as a function of polar angle θ and azimuth ϕ.

(C1, C2) in each event (we assign to each cluster a four-momentum (Eu, E), E being the cluster energy and u the unit vector pointing from the event vertex to the cluster center). We measure P_T to be 6 GeV/c on the average, of which at least 3 GeV/c are of instrumental nature (non-inclusion of large angle fragments in the cluster, energy resolution, edge effects, etc.).

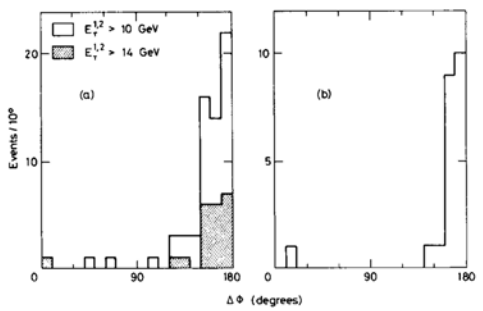


Fig. 5. (a) Azimuthal separation between C1 and C2 (see text) for $E_T^{1,2} > 10$ and 14 GeV. (b) Azimuthal separation between C1 and the forward/backward sector having $E_T > 5$ GeV for $E_T^1 > 10$ GeV and $E_T^2/E_T^1 < 0.4$ (see text).

The above observations support the interpretation of S_{JJ} as a sample of two-jet events resulting from a hard parton collision. We remark however that the spectacular configuration illustrated in fig. 4 is not representative of the whole sample. As shown in fig. 3a the two-jet system accounts for only a fraction of ΣE_T. The rest of the transverse energy in the event, $\widetilde{E}_T$, is distributed among clusters, of which typically 2 to 3 are in excess of 1 GeV. Their detailed study is beyond the scope of the present report. We simply remark that they are only weakly correlated with the jet directions and that their multiplicity and transverse energy distributions are the same as in events having $\Sigma E_T = \widetilde{E}_T$.

Given the presence of relatively abundant and hard clusters accompanying the two-jet system, we further ascertain the emergence of a two-jet (as opposed to multi-jet) structure by measuring the dependence upon ΣE_T of the ratios $r_{21} = E_T^2/E_T^1$ and $r_{32} = E_T^3/E_T^2$. As ΣE_T increases, r_{21} increases and r_{32} decreases (fig. 3b), again illustrating the dominance of two-jet events for ΣE_T exceeding ≃60 GeV.

Downloaded from https://www.cambridge.org/core. UNIVERSIDAD AUTONOMA METROPOLITANA, on 19 Nov 2026 at 11:01:57, subject to the Cambridge Core terms of use, available at https://www.cambridge.org/core/terms. https://doi.org/10.1017/9780511609923.012

7. Inclusive jet production. There are 59 events containing at least one cluster with $E_T > 20$ GeV. The evaluation of the inclusive jet production cross section from these events requires the knowledge of the detector acceptance and luminosity.

The detector acceptance is obtained from a Monte Carlo simulation that generates jets with the E_T-distribution given in ref. [6], superimposed on a system of soft hadrons accounting for the remaining fraction of $\sqrt{s}$. The jets fragment into hadrons with an average transverse momentum of 0.45 GeV/c with respect to the jet axis according to a fragmentation function of the form $(1-x)^2/x$ (x is the fractional momentum of the fragment along the jet axis). All of these hadrons (assumed to be charged and neutral pions only) are then followed into the calorimeters to generate a pattern of energy depositions. Both the longitudinal and lateral shower developments as well as the energy resolution are taken into account.

The data generated by the Monte Carlo simulation undergo the same analysis chain as the real data. In particular, we find that the distribution of cluster size in the Monte Carlo data is very similar to that of the real data, indicating that both hadronic fragmentation and shower developments are correctly described in the simulation program.

The comparison of the E_T-distribution of the Monte Carlo data with that used as an input provides the correction function $\alpha(E_T)$ by which the observed cross section must be divided to obtain the jet inclusive cross section. We have checked that varying some of the analysis parameters, in particular those related to the cluster definition, changes both the observed E_T distribution and $\alpha(E_T)$ but the correct cross section always varies by less than 10%. The function $\alpha(E_T)$ varies by less than a factor of 2 over the range $20 < E_T < 60$ GeV.

The integrated luminosity is obtained by counting the total number of minimum bias events which occurred during data taking. From the fluctuations measured during different running conditions we assign an uncertainty of ±17% to its value. An additional uncertainty results from the fact that, as already mentioned, the trigger to record large-E_T events required a coincidence with a pair of small angle charged secondaries. This requirement introduces a bias which may affect both the absolute magnitude of the cross section and its E_T-dependence.

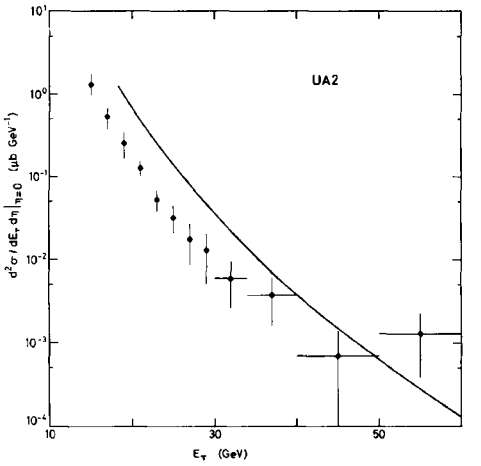


Fig. 6. Inclusive jet production cross section. The solid line (ref. [6]) uses $\Lambda = 0.5$ GeV while $\Lambda = 0.15$ GeV would bring the calculated rates in better agreement with the data. However various uncertainties preclude a determination of Λ from the data [13].

Fig. 6 shows the cross section for inclusive jet production as a function of the jet transverse energy E_T. The errors shown are only statistical. There is an overall uncertainty of ±20% in the vertical scale reflecting the uncertainties in the knowledge of the total luminosity and in the Monte Carlo calculated acceptance. An uncertainty of ±2.5% in the E_T-scale, reflecting the calorimeter energy calibration uncertainties, results in an additional vertical uncertainty of ±20%. From a visual scan of the events the contribution from sources other than $\bar{p}p$ collisions is estimated to be <10%, independent of E_T.

Our measured cross section is at a level comparable with the QCD calculation of Horgan and Jacob [6], which is also shown in fig. 6. In the framework of this model, inclusive jet production is dominated by gluon–gluon scattering in the kinematical region of this experiment.

We finally note that the possible merging of two high E_T clusters produced with a small angular separation may increase the measured cluster energy by as much as 2 GeV on the average. This effect is not accounted for in ref. [6] where jet fragmentation is ignored.

Downloaded from https://www.cambridge.org/core. UNIVERSIDAD AUTONOMA METROPOLITANA, on 19 Nov 2026 at 11:01:57, subject to the Cambridge Core terms of use, available at https://www.cambridge.org/core/terms. https://doi.org/10.1017/9780511609923.012

Volume 118B, number 1, 2, 3 PHYSICS LETTERS 2 December 1982

8. Conclusion. We have observed that events with a large transverse energy (in excess of ≃60 GeV) in a rapidity interval of two units around 90° have a dominant two-jet structure at $\sqrt{s}$ = 540 GeV. This is in strong contrast with the situation at $\sqrt{s}$ = 24 GeV [11]. The inclusive jet production cross section is measured at a level similar to that predicted by QCD calculations [6]. A sample of two-jet events has been studied and observed to feature properties characteristic of hard scattering of partons. This observation provides the first evidence for highly collimated jets produced in hadron collisions.

We deeply acknowledge the help of the technical staffs of the Institutes collaborating in UA2 and particularly that of the CERN staff who assembled the central calorimeter and its associated electronics: F. Bourgeois and his team, L. Bonnefoy, J.-M. Chapuis, Y. Cholley, G. Gurrieri and A. Sigrist. Financial support from the Danish Natural Science Research Council to the Niels Bohr Institute group and from the Schweizerischer National fonds zur Förderung der wissenschaftlichen Forschung to the Bern group are acknowledged.

References

[1] S.M. Berman, J.D. Bjorken and J.B. Kogut, Phys. Rev. 4D (1971) 3388.
[2] For reviews see: K. Hansen and P. Hoyer, eds., Jets in high energy collisions, Phys. Scr. 19 (1979);
P. Darriulat, Ann. Rev. Nucl. Part. Sci. 30 (1980) 159.
[3] M.G. Albrow et al., Nucl. Phys. B160 (1979) 1;
A.L.S. Angelis et al., Phys. Scr. 19 (1979) 116;
A.G. Clark et al., Nucl. Phys. B160 (1979) 397;
D. Drijard et al., Nucl. Phys. B166 (1980) 233.
[4] For a review see: P. Söding and G. Wolf, Ann. Rev. Nucl. Part. Sci. 31 (1981) 231.
[5] The Staff of the CERN $\bar{p}p$ project, Phys. Lett. 107B (1981) 306.
[6] R. Horgan and M. Jacob, Nucl. Phys. B179 (1981) 441.
[7] K. Alpgård et al., Phys. Lett. 107B (1981) 310.
[8] M. Banner et al., Phys. Lett. 115B (1982) 59;
The UA2 Collab., First results from the UA2 experiment at the SPS $p\bar{p}$ collider, presented XIIIth Intern. Symp. on Multiparticle Dynamics (Volendam, The Netherlands, June 1982).
[9] A.G. Clark, Proc. Intern. Conf. on Instrumentation for Colliding beam physics (SLAC, 1982);
The UA2 Collab., Status and first results from the UA2 experiment, presented 2nd Intern. Conf. on Physics in Collission (Stockholm, Sweden, June 1982);
F. Bonaudi et al., in preparation.
[10] V. Hungerbühler, Proc. Topical Conf. on the Applications of microprocessors to high energy physics experiments, CERN 81-07 (1981) p. 46.
[11] C. de Marzo et al., Phys. Lett. 112B (1982) 173;
M. Arenton et al., Evidence for jets from a transverse energy triggered calorimeter experiment at Fermilab, Contrib. XXIst Intern. Conf. on High Energy Physics (Paris, France, July 1982);
B. Brown et al., Properties of high transverse energy hadronic events, NAL preprint Fermilab-Conf. – 82/34 – Exp. (1982).
[12] M. Jacob, in: Proton–antiproton collider physics (1981), AIP Conf. Proc. nr. 85, p. 651;
H.U. Bengtsson and T. Åkesson, Transverse energy distribution and hard constituent scattering in hadronic collisions, contribution XXIst Intern. Conf. on High Energy Physics (Paris, July 1982).
[13] M. Jacob, private communication.

Downloaded from https://www.cambridge.org/core. UNIVERSIDAD AUTONOMA METROPOLITANA, on 19 Nov 2026 at 11:01:57, subject to the Cambridge Core terms of use, available at https://www.cambridge.org/core/terms. https://doi.org/10.1017/9780511609923.012